AD NUMBER

AD844655

LIMITATION CHANGES

TO:

Approved for public release; distribution is unlimited.

FROM:

Distribution authorized to U.S. Gov't. agencies and their contractors; Critical Technology; MAR 1968. Other requests shall be referred to Air Force Technical Applications Center, Washington, DC. This document contains export-controlled technical data.

AUTHORITY

usaf, ltr, 28 feb 1972

RAYLEIGH WAVE DISCRIMINATION TECHNIQUES BETWEEN UNDERGROUND EXPLOSIONS AND EARTHQUAKES

1 March 1968

Prepared for

AIR FORCE TECHNICAL APPLICATIONS CENTER
Washington, D. C.

By

L. S. Turnbull, Jr.
TELEDYNE, INC.

D. G. LAMBERT
TELEDYNE, INC.

C. A. Newton
PENNSYLVANIA STATE UNIVERSITY

Under

Project VELA UNIFORM

Sponsored By

ADVANCED RESEARCH PROJECTS AGENCY
Nuclear Test Detection Office
ARPA Order No. 624

RAYLEIGH WAVE DISCRIMINATION TECHNIQUES BETWEEN UNDERGROUND EXPLOSIONS AND EARTHQUAKES

SEISMIC DATA LABORATORY REPORT NO. 211

AFTAC Project No.:	VELA T/6702
Project Title:	Seismic Data Laboratory
ARPA Order No.:	624
ARPA Program Code No.:	8F10
Name of Contractor:	TELEDYNE, INC.
Contract No.:	F33657-68-C-0945
Date of Contract:	2 March 1968
Amount of Contract:	$ 1,251,000
Contract Expiration Date:	1 March 1969
Project Manager:	Royal A. Hartenberger (703) 836-7647

P. O. Box 334 Alexandria, Virginia

AVAILABILITY

This research was supported by the Advanced Research Projects Agency, Nuclear Test Detection Office, under Project VELA-UNIFORM and accomplished under the technical direction of the Air Force Technical Applications Center under Contract F 33657-68-C-0945

TABLE OF CONTENTS

	Page No.
ABSTRACT	
INTRODUCTION	1
Methods of Analysis	1
A. ARZ	1
B. ERZ	2
C. REF	2
Program Description	3
DATA ANALYSIS AND RESULTS	5
CONCLUSIONS	10
RECOMMENDATIONS	10
REFERENCES	

LIST OF ILLUSTRATIONS

TABLES:

I. Event Epicenter Listing

II. Comparison of Data from Matched Filter and AR Programs

FIGURES:

1. Flow chart for Rayleigh wave discrimination program. Output includes ARZ, ERZ, REF and signal spectrum.

2. a. Fallon Eq - ARZ vs. Distance

   b. Fallon Eq - ARZ vs. Distance. Normalized to surface wave magnitude $M_V = 4.0$.

   c. Fallon Eq - ERZ vs. Distance.

   d. Fallon Eq - ERZ vs. Distance. Normalized to surface wave magnitude $M_V = 4.0$.

3. a. Shoal - ARZ vs. Distance

   b. Shoal - ARZ vs. Distance. Normalized to surface wave magnitude $M_V = 4.0$.

   c. Shoal - ERZ vs. Distance

   d. Shoal - ERZ vs. Distance. Normalized to surface wave magnitude $M_V = 4.0$.

4. a. Geurrero, Mexico Eq. - ARZ vs. Distance. Normalized to surface wave magnitude $M_V = 4.0$.

   b. Guerrero, Mexico Eq. - ERZ vs. Distance. Normalized to surface wave magnitude $M_V = 4.0$.

   c. Guerrero, Mexico Eq. - REF vs. Distance. No structure correction. Normalized to surface wave magnitude $M_V = 4.0$.

   d. Guerrero, Mexico Eq. - REF vs. Distance. Structure correction. Normalized to surface wave magnitude $M_V = 4.0$.

   e. Energy Density vs. Period at FK-CO.

   f. Energy Density vs. Period at UBO.

FIGURES:

5. a. Komandorsky Islands Eq. I - ARZ vs. Distance. Normalized to surface wave magnitude M_v = 4.0.

   b. Komandorsky Islands Eq. I - ERZ vs. Distance. Normalized to surface wave magnitude M_v = 4.0.

   c. Komandorsky Islands Eq. I - REF vs. Distance. No structure correction. Normalized to surface wave magnitude M_v = 4.0.

   d. Komandorsky Islands Eq. I - REF vs. Distance. Structure correction. Normalized to surface wave magnitude M_v = 4.0.

6. a. Bourbon - ARZ vs. Distance.

   b. Bourbon - ARZ vs. Distance. Normalized to surface wave magnitude M_v = 4.0.

   c. Bourbon - ERZ vs. Distance. Normalized to surface wave magnitude M_v = 4.0.

   d. Bourbon - REF vs. Distance. Structure correction. Normalized to surface wave magnitude M_v = 4.0.

7. a. Long Shot - ARZ vs. Distance. Normalized to surface wave magnitude M_v = 4.0.

   b. Long Shot - ERZ vs. Distance. Normalized to surface wave magnitude M_v = 4.0.

   c. Long Shot - REF vs. Distance. Structure correction, Normalized to surface wave magnitude M_v = 4.0.

8. a. Andreanof Is. Eq. - ARZ vs. Distance. Normalized to surface wave magnitude M_v = 4.0.

   b. Andreanof Is. Eq. - ERZ vs. Distance. Normalized to surface wave magnitude M_v = 4.0.

9. a. Bilby - ARZ vs. Distance - Normalized to surface wave magnitude M_v = 4.0.

   b. Bilby - ERZ vs. Distance - Normalized to surface wave magnitude M_v = 4.0.

10. a. Calif-Nevada Border Eq. - ARZ vs. Distance. Normalized to surface wave magnitude M_v = 4.0.

    b. Calif-Nevada Border Eq. - ERZ vs. Distance. Normalized to surface wave magnitude M_v = 4.0.

FIGURES:

11. a. Komandorsky Islands Eq. II - ARZ vs. Distance. Normalized to surface wave magnitude M_v = 4.0.

    b. Komandorsky Islands Eq. II - ERZ vs. Distance. Normalized to surface wave magnitude M_v = 4.0.

12. ARZ (At 1000 km) vs. P-wave magnitude (m_b) for 12 events.

13. ARZ (At 1000 km) vs. Rayleigh wave magnitude (M_v) for 13 events.

14. ERZ (At 1000 km) vs. P-wave magnitude (m_b) for 12 events.

15. ERZ (At 1000 km) vs. Rayleigh wave magnitude (M_v) for 13 events.

16. Comparison of data for synthetic case using matched filter and AR program - Measured Signal Level vs. Signal Input Level (S/N).

ABSTRACT

Discrimination between underground nuclear explosions and shallow earthquakes using the vertical component of the Rayleigh wave is achieved using several techniques. This analysis includes the previous developed area under the Rayleigh wave (ARZ), the newly applied total energy (ERZ), and the total energy transported across a unit width of the waveguide by the Rayleigh wave (REF). Results for several explosions and earthquakes of varying magnitudes are presented. Evaluation of these techniques and their applicability in an automated discrimination program is discussed. An attempt is made to incorporate a matched filter approach for weak signals.

INTRODUCTION

The objective of this study is to examine possible discrimination techniques using the vertical component of the Rayleigh wave. The use of surface waves in a discrimination process was originally discussed by Brune, Espinosa, and Oliver (1963) with their introduction of the AR diagnostic (the area included in the envelope of the surface waves of a seismogram). Subsequent investigation has shown that better results are obtained using only the vertical component of the Rayleigh wave in the AR process. With this tool as the basic discriminant, and with the idea of obtaining optimum results for the time invested, modifications have been made to the AR process, and new discriminants have been tried. A program has been written which yields results for each discriminant, enabling comparisons to be made readily. In the following paragraphs, a theoretical description is included for each tool, the results for each discriminant on actual data is given, and the program which performs these calculations is described.

Methods of Analysis

ARZ: This was originally defined as the area within the envelope of the vertical component of the Rayleigh wave recorded on a standard instrument at standard magnification. This quantity has no physical meaning. Its motivation was founded on the fact that it was easy to measure manually by tracing out the envelope and then using a planimeter to obtain the area.

In our effort to automate this process and bring the speed of a computer into play, computing the envelope was found to be cumbersome. Instead, using the area obtained by integrating the absolute value of the trace amplitude was found to be more efficient.

Mathematically, the definition of the area under the vertical component of the Rayleigh wave that is now being used is

$$ARZ = \int_{T_1}^{T_2} |f(t)|dt$$

where $f(t)$ is the seismogram trace and T_2-T_1 the group velocity window we are examining.

ERZ: By definition, ERZ is proportional to the total energy in the Rayleigh wave:

$$ERZ = \int_{T_1}^{T_2} f^2(t)dt.$$

The motivation for this discriminant can be found in the need to develop some easily calculable quantity which has a physical interpretation, and has better discrimination ability than ARZ.

REF: This quantity is defined as the Rayleigh energy flux, the energy transported across a unit width of the wave guide by the Rayleigh wave. In a perfectly elastic medium the energy flux out of any closed surface containing the source is equal to the energy injected by the source into the medium. Therefore, REF, when corrected for geometrical spreading, shows effects of only the crustal filtering, i.e., scattering and absorption losses, and the source radiation pattern.

$$REF = \int_{-\infty}^{\infty} U(\omega)\omega^2 \int_0^{\infty} \rho(z) \left[\bar{Q}^2(z,\omega) + \bar{W}^2(z,\omega)\right] W^2(0,\omega)dzd\omega$$

where

U: group velocity

$\bar{Q}$: normalized radial displacement

$\bar{W}$: normalized vertical displacement

$W(0,\omega)$: observed surface vertical displacement

ρ: density

REF - W(ω): This quantity is the structure correction for the REF, which takes into account the effect of structure for a particular recording station. If the structure under the recording station is known, then the normalized spectral energy density, E_n, may be calculated using Harkrider's dispersion program.

$$E_n = \omega^2 \int_0^\infty \rho(z) \left[\bar{Q}^2(z,\omega) + \bar{W}^2(z,\omega) \right] dz$$

The structure correction factor can be defined as

$$K(\omega) = U(\omega) E_n(\omega)$$

Therefore, we can write the Rayleigh energy flux as

$$REF = \int_{\omega_1}^{\omega_2} K(\omega)\ W_0^2\ (\omega)\ d\omega,$$

where the surface wave packet is band-limited ($\omega_1 < \omega < \omega_2$) as a consequence of the source excitation and the crustal and instrumental filtering.

Program Description

A flow diagram of the AR program is shown in Figure 1. It shows what steps are required to calculate ARZ, ERZ, and REF; in particular, what spectra are calculated and where the instrument response and noise corrections are applied. The following paragraphs give a modular description of the program.

Tape Input: The entire trace of the first seismogram is read. The program will handle up to 16000 points.

Card Input: Besides providing the event identification information, options and controls for the tape input are also given (i.e., the record start time can be corrected).

Preprocessed Time Series: In this module, the trace is prepared for computation by correcting for static magnification,

decimating, detrending, tapering, and bandpass filtering from 0.02 to 0.10 cps.

Computation:

ARZ - The area under both the signal and the noise sample are calculated using the QUADR subroutine (Simpson's rule integration), and then the area of the noise is subtracted from that of the signal.

ERZ - First, the spectral amplitude and the phase of the signal and noise samples are computed using the subroutine GRTZSPEC, and the phase is unwound. Then the spectra are corrected for system response. Finally, the spectra of the noise is subtracted from that of the signal and ERZ is calculated (see definition).

REF - Using the spectra calculated for ERZ, the Rayleigh energy flux is computed (see definition). This is modified by the station structure corrections as given by Harkrider's program.

Output:

Printout: Besides the event identification information, several plots are furnished:

1. Signal sample (time series).
2. Noise time series.
3. Signal amplitude spectra corrected for system response and static magnification.
4. Noise amplitude spectra corrected for system response and static magnification.
5. Signal amplitude spectra corrected for noise.
6. Particle velocity spectra corrected for system and noise response.

Also, values are given for the AR of the signal, the AR of the noise, the AR of the signal corrected for noise (ARZ), the ERZ of the signal corrected for noise, the REF of the signal corrected for structure, and the Rayleigh wave magnitude (M_v) of the signal.

Binary Save Tape: With the event identification, the

amplitude and phase spectrum will be saved of the resultant (signal less noise) and noise.

DATA ANALYSIS AND RESULTS

The ability of AR to discriminate between explosions and shallow earthquakes has been demonstrated by several authors. The purpose of this work is to improve the discrimination ability of AR and other parameters with a minimum of computing effort.

The bulk of the time by other authors and in this investigation was spent attempting to apply the proper corrections for distance, azimuth, and attenuation in order to eliminate path effects and to try to make the discriminant a diagnostic of the source only. This can be graphically demonstrated if the scatter can be reduced for a particular event in a plot of ARZ versus distance.

A correction which has been found to be particularly fruitful is the normalization of ARZ at all stations to a fixed surface wave magnitude. By using the surface wave magnitude, we only need to deal with the vertical component of Rayleigh wave and do not need to examine the short-period body wave train. The surface wave magnitude is defined by

$$M_v = \text{Log } A/_T + 1.66 \text{ Log } \Delta^\circ - 0.18$$

where

1) $A/_T$ = maximum particle velocity peak to peak, between T = 17 and 30 seconds
2) Δ = distance in degrees.

The normalization is accomplished by:

$$(\overline{M}_v - M_{v_i}) = \overline{\text{Log}(A/_T)} - \text{Log}(A/T)_i + 1.66(\overline{\text{Log}\Delta} - \text{Log } \Delta_i)$$

therefore,

$$R = \text{anti-log } (\overline{M}_v - M_{v_i})$$

where $\overline{M}_v$ = average Rayleigh magnitude for the set of records

analyzed, i.e., $\bar{M}_v = 1/n \sum_{i=1}^{n} M_{v_i}$

Therefore, R · AR = normalized value of AR to a given $\bar{M}_v$.

Figures 2 and 3 give illustrations on the application of this normalization to an earthquake (Fallon) and an explosion (Shoal). The uncorrected plot of ARZ versus distance for 10 stations is shown in Figure 2a with the normalized values of ARZ versus distance shown in 2b. The reduction in the scatter of points due to the normalization is quite obvious.

In an effort to place a physical significance on the measurements, the parameter ERZ was developed (see definition). The uncorrected plot of ERZ versus distance for the Fallon earthquake is shown in Figure 2c, and the normalized plot is shown in Figure 2d. Again the reduction in scatter of the points is quite obvious. The normalization of ERZ values is accomplished by the following:

since $A^2 \simeq E$ (i.e., Amplitude$^2 \simeq$ Energy)

and

$$2\left[\bar{M}_v - \bar{M}_{v_i}\right] = \overline{\text{Log}(A/T)} - \text{Log}(A/_T) + 3.32(\overline{\text{Log}\Delta} - \text{Log}\Delta_i)$$

Therefore,

$$R_E = \text{anti-log } 2\left[\bar{M}_v - M_{v_i}\right]$$

and ERZ · R_E = normalized value of ERZ to an $\bar{M}_v$.

A similar set of figures is shown for the Shoal explosion. The uncorrected and normalized values for ARZ and ERZ is shown in Figure 3a through 3d. The reduction of point scatter is again quite significant.

With the large reduction in point scatter possible due to the normalization to M_v, further reduction in the scatter was thought possible with the inclusion of a station structure correction. The parameter REF, the energy transported across a unit width of the wave guide by the Rayleigh wave, was

developed at this point (see definition). Figures 4 and 5 illustrate the use of REF and the effect of the structure correction. Figures 4a through 4f deal with a Guerrero, Mexico, earthquake. (For identification information on each event discussed see Table I - Event Epicenter Listing). Plots similar to those for Fallon and Shoal of ARZ and ERZ normalized to M = 4.0 are given in Figures 4a and 4b. In Figure 4c, the REF normalized to M_v = 4.0 is plotted versus distance with no structure correction for seven stations. The standard deviation of a least squares straight line is SD = $\pm$ 0.077. In Figure 4d we have the sample plot except that a structure correction has been applied to the same seven stations. The standard deviation of a least squares straight line is SD = $\pm$ 0.068. A comparison of the results from Figures 4c and 4d imply that the structure correction is of secondary importance, since the overall reduction in point scatter is quite negligible. If one is willing to say it was possible that the structures for the stations used were similar, then only an examination of Figures 4e and 4f is needed. For stations FK-CO and UBO, plots of energy density versus period are shown together with group and phase velocity curves. The energy densities are quite dissimilar. Therefore, one can only conclude that large perturbations in structure have a negligible, if noticeable, affect on the REF parameter.

A similar set of plots for a Komandorsky Islands earthquake of 8 February 1965 shows the same results. Figures 5a and 5b give normalized plots of ARZ and ERZ. The normalized REF with no structure correction is shown in Figure 5c, with the standard deviation for a least squares fit SD = $\pm$ 0.094. The normalized REF with structure correction is shown in Figure 5d, with a standard deviation SD = $\pm$ 0.115. For this event, the structure correction produced worse results than the REF computation with no structure correction. This result further demonstrates the lack of effectiveness present in the structure correction.

Figures 6 through 11 give results similar to those discussed for Figures 2 through 5. They cover the results for three shots

(Bourbon, Long Shot, and Bilby), and for three earthquakes (Andreanof Islands, California-Nevada Border, Komandorsky Islands of 14 February 1965).

Composite plots of the data for the events previously discussed are given in Figures 12 through 15. Figures 12 and 14 show ARZ and ERZ respectively, taken at a standard distance of 1000 km and plotted versus body-wave magnitude (m_b). The separation between explosions and shallow earthquakes is what we expect from previously published results, with distinct groupings of the data. But the results shown in Figures 13 and 15 do not have this distinct separation. In these figures, ARZ and ERZ, taken at a standard of 1000 km, are plotted versus surface wave magnitude (M_v). Although the explosions generally have a lower ARZ or ERZ for a particular magnitude, there is no separation as before.

An explanation for this lack of separation can be found if we examine our definition of M_v and look in closer detail at the spectra for each event. As defined previously, M_v is calculated by picking the maximum amplitude, peak to peak, which occurs between T = 17 and 30 seconds. Hence, we are averaging the long period energy over the entire interval. By doing this, we have lost some information generally inherent in the wave trains for explosions and earthquakes. Because of the lack of shear wave radiation produced by explosive sources, the energy in the long period Rayleigh waves should be reduced, with most of the energy contained in the shorter periods. For earthquakes, however, more energy should be contained in the longer-period Rayleigh waves.

Finally, an attempt has been made to extend the use of ARZ and ERZ to low signal-to-noise ratios with the use of a matched filter. The ratio of ARZ's or the square root of the ratio of ERZ's for different events occurring at the same location corresponds to the value of the parameter $\hat{a}$ obtained from the matched filter analysis (Alexander and Rabenstine, 1967),

where

$$\hat{a} = \sum_t x(t+\tau)v(t) / \sum_t y^2(t),$$

x(t) being the test case and y(t) the known waveform.

A comparison of the ratios with â was made for the two Greenland Sea Events of 18 November 1966 studied by Alexander and Rabenstine. These events occurred approximately 40 minutes apart at the same location, the first having M_v of 3.6 and the second having M_v of 4.8. A summary of the ratios obtained is given in Table II.

Good agreement exists between the square root of the ratio of ERZ's and â. For those values for which a substantial difference exists, an explanation can be found in the method used to correct for noise, which is not the same for both. The ERZ is corrected for noise by a simple subtraction of spectra, while the value for the noise correction used in calculating â is the rms n(t) . The ratio of the ARZ's of the signal alone (ARZS) also compares favorably with â, but the ratio of ARZ's corrected for noise are in poor agreement. The latter ratio is generally much lower in a station-by-station comparison, indicating that the noise sample used to correct ARZ is overestimated especially at low S/N ratios, with the good possibility of producing a negative ARZ.

A graphic demonstration of the compatability of these ratios with â is shown in Figure 16. A synthetic case was produced where an actual signal is buried in a noise sample to produce known signal-to-noise ratios. This signal is then used as a matched filter. These same signal-noise combinations were then processed by the AR program. This case also demonstrates that the best overall agreement is obtained using the square root of the energy ratio. But more work is needed to completely understand the effect of the noise corrections on the ratios, especially for low S/N.

CONCLUSIONS

On the basis of this investigation of discrimination techniques using the vertical component of the Rayleigh wave we conclude that:

1. In plotting ARZ, ERZ, or REF versus Rayleigh wave magnitude for a particular event, the point scatter is significantly reduced by the normalization to a particular M_V;

2. The structure correction applied to the REF calculation has little if any effect;

3. Plots of ARZ and ERZ versus body wave magnitude yield greater discrimination between explosions and shallow earthquakes than plots using the surface wave magnitude;

4. The matched filter can be used to extend the ERZ parameter to low signal-to-noise ratios with reasonable agreement between the two parameters ($\sqrt{ERZ_{2/ERZ_1}}$ and â) where they can be compared.

RECOMMENDATIONS:

The parameter which yields the greatest discrimination is ERZ. In plots versus body-wave magnitude, the separation is of the same order as those using ARZ. Although it takes slightly more time to calculate than ARZ, this is more than offset by the greater accuracy in the noise correction, the good agreement in comparisons with the matched filter, and the fact that this parameter has physical significance. Although the REF parameter had a more satisfying physical interpretation, the negligible improvement when the structure correction is applied leaves something to be desired for the amount of analysis and computer time needed. Therefore, ERZ should be used as a basis for discrimination programs and further investigations into the discrimination problem. These investigations should include an examination of the matched filter and the ERZ and ARZ ratios for low S/N.

REFERENCES

Alexander, S.S., and D.B. Rabenstine, 1967, Rayleigh wave signal to noise enhancement for a small teleseism using LASA, LRSM, and observatory stations, SDL Report No. 194, 21 August.

Alexander, S.S., and D.B. Rabenstine, 1967, Detection of surface waves from small events at teleseismic distances, SDL Report No. 175, 1 March.

Bracewell, R., 1965, The Fourier transform and its applications, New York, McGraw-Hill Book Company.

Brune, J., A. Espinosa, and J. Oliver, 1963, Relative excitation of surface waves by earthquakes and underground explosions in the California-Nevada region, Jour. Geoph. Res., Vol. 68, No. 11.

De Noyer, J., 1958, Determination of the energy in body and surface waves (Part I), Bull. Seis. Soc. Amer., vol. 48, No. 5.

De Noyer, J., 1949, Determination of the energy in body and surface waves (Part II), Bull. Seis. Soc. Amer., vol. 49, No. 1.

Dugundju, J., 1958, Envelopes and pre-envelopes of real waveforms, Trans. IRE, Vol. IT-4, p. 53-57.

McCowan, D.W., 1967, Finite Fourier transform theory and its application to the computation of convolutions, correlations, and spectra, SDL Report No. 168 (Revised), 17 October.

TABLE I

Event Epicenter Listing

Date	Area	Latitude	Longitude	Origin Time	Depth	Body Wave Magnitude	Rayleigh Wave Magnitude
13 Sept. 1963	Bilby N.T.S.	37°03.633'N	116°01.30'W	17:00:00.1 Z	0.76Km	5.62	3.88±0.27
26 Oct. 1963	Shoal-Sand Springs Range, Nevada	39°12.017'N	118°22.817'W	17:00:00.1 Z	0.37Km	4.8	2.43±0.39
29 Oct. 1965	Long Shot-Amchitka Island, Aleutians	51°26.294'N	179°10.950'E	21:00:00.1 Z	0.76Km	5.97±0.48	4.13±0.40
20 Jan. 1967	Bourbon N.T.S.	37°05.984'N	116°00.233'W	17:40:04.4 Z	0.56Km	4.66	3.32±0.49
20 July 1962	Fallon, Nevada Eq.	39°38.883'N	118°12.667'W	09:02:08.3 Z	20Km	4.1	2.86±0.33
8 Feb. 1965	Komandorsky Eq.	55°06'N	165°42'W	15:46:49.9 Z	40Km	5.6	5.82±0.15
14 Feb. 1965	Komandorsky Eq.	55°06'N	165°36'W	17:01:13.9 Z	20Km	5.0	3.93±0.20
22 Nov. 1965	Andreanof Eq.	51°18'N	179°48'W	20:25:30.4 Z	40Km	5.9	5.55±0.17
18 Nov. 1966	Greenland Sea Eq.	73°24'N	06°48'E	18:07:54.0 Z	33Km	4.6	3.60±0.46
18 Nov. 1966	Greenland Sea Eq.	73°24'N	06°48'E	18:48:43.9 Z	33Km	4.9	4.82±0.30
2 Mar. 1967	California-Nevada Brd. Eq.	36°18'N	117°42'W	14:12:49.1 Z	14Km	3.67	2.54±0.63
13 Apr. 1967	Guerrero, Mexico Eq.	18°30'N	100°12'W	19:59:51.9 Z	86Km	5.6	4.78±0.40

TABLE II

Comparative Data From Matched Filter and AR Programs

Greenland Sea Events 18 Nov. 1966

Station Code	$\frac{ARZ_1}{ARZ_2}$	$\frac{ARZS_1}{ARZS_2}$	Matched Filter $\hat{a}$	$\frac{ERZ_1}{ERZ_2}$
HN-ME	0.0074	0.2380	0.0370	0.0813
RK-ON	0.0445	0.0663	0.0655	0.0557
PG-BC	0.0528	0.0851	0.0775	0.0708
KC-MO	0.0349	0.0711	0.0535	0.0458
MO-ID	0.0458	0.0865	0.0720	0.0656
UBO	-0.0700	0.0700	0.0330	0.0112
AX2AL	0.0234	0.0805	0.0465	0.0600
EU2AL	-0.0006	0.0870	0.0490	0.0448
WMO	0.0443	0.0728	0.0565	0.0510
BE-FL	0.0321	0.1765	0.0370	0.0775
JE-LA	0.0025	0.1021	0.0465	0.0837
MN-NV	0.0459	0.1586	0.0430	0.0960

Notes:
Subscript 1: Greenland Sea Eq. 18:07:54.0 Z
Subscript 2: Greenland Sea Eq. 18:48:43.9 A
ARZ_1/ARZ_2: Ratio of ARZ'S corrected for noise
$ARZS_1/ARZS_2$: Ratio of ARZ'S not corrected for noise
ERZ_1/ERZ_2: Ratio of ERZ'S corrected for noise

EARTHQUAKE GUERRERO MEXICO

13 APRIL 1967, m = 5.6, h = 86 km, MN-NV, Δ = 2811 km

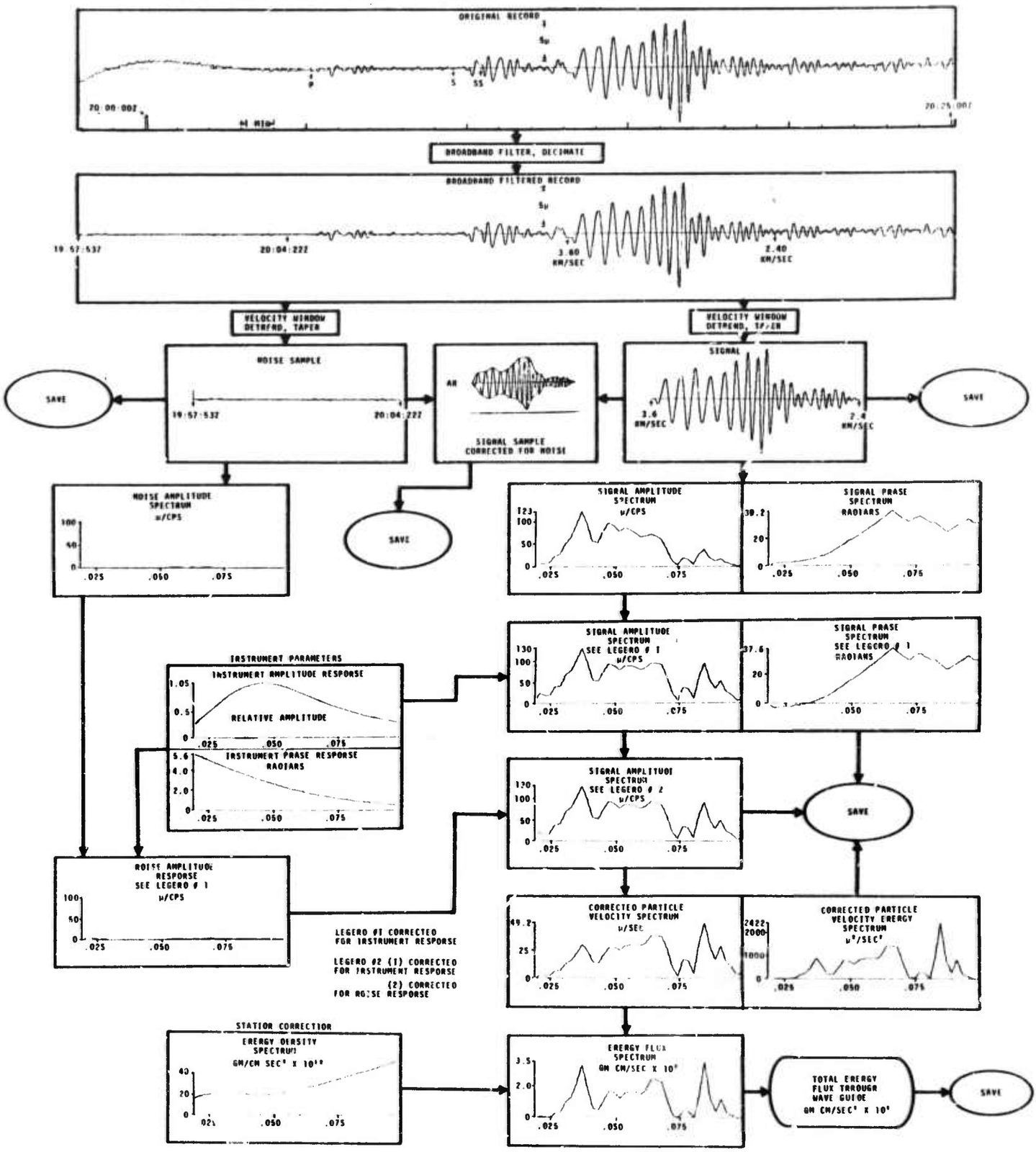

Figure 1. Flow chart for Rayleigh wave discrimination program

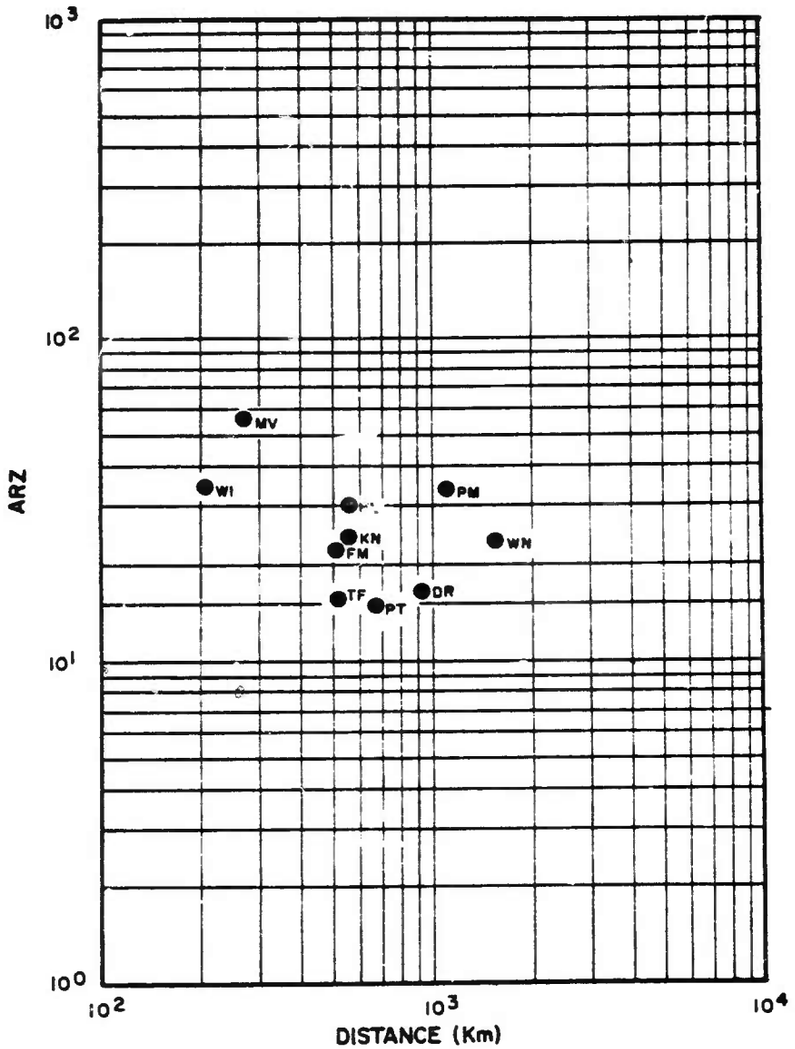

Figure 2a. Fallon Eq. - ARZ vs. Distance.

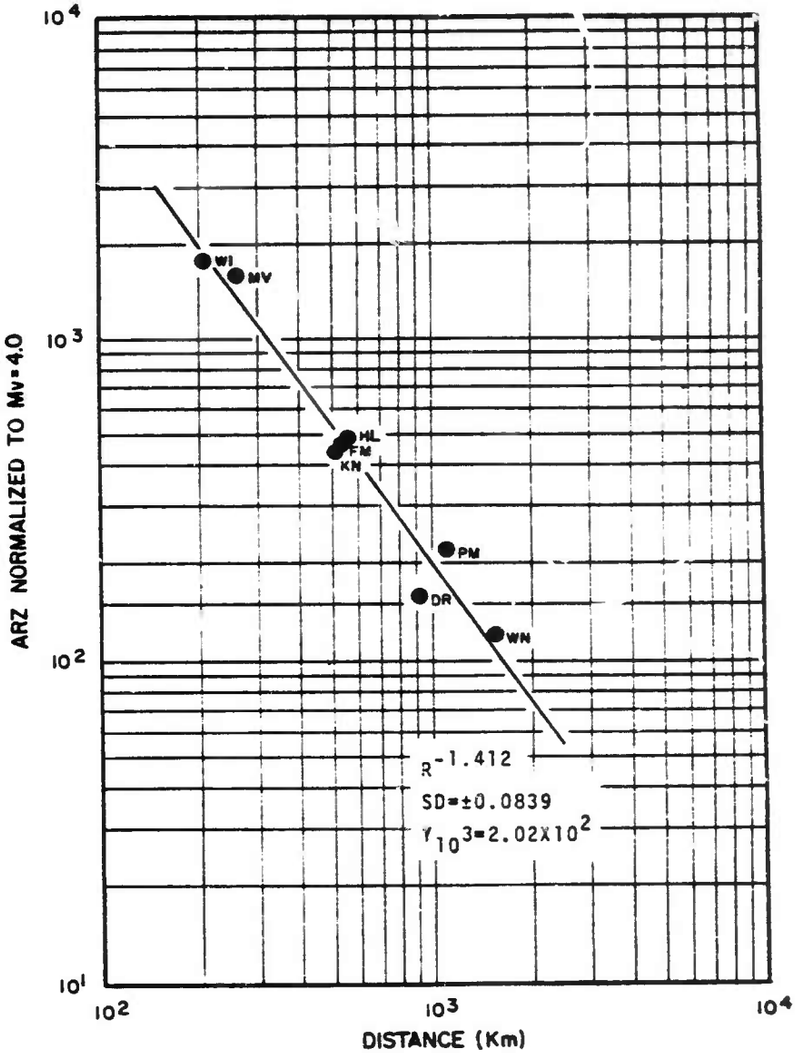

Figure 2b. Fallon Eq. - ARZ vs. Distance. Normalized to surface wave magnitude M_V = 4.0.

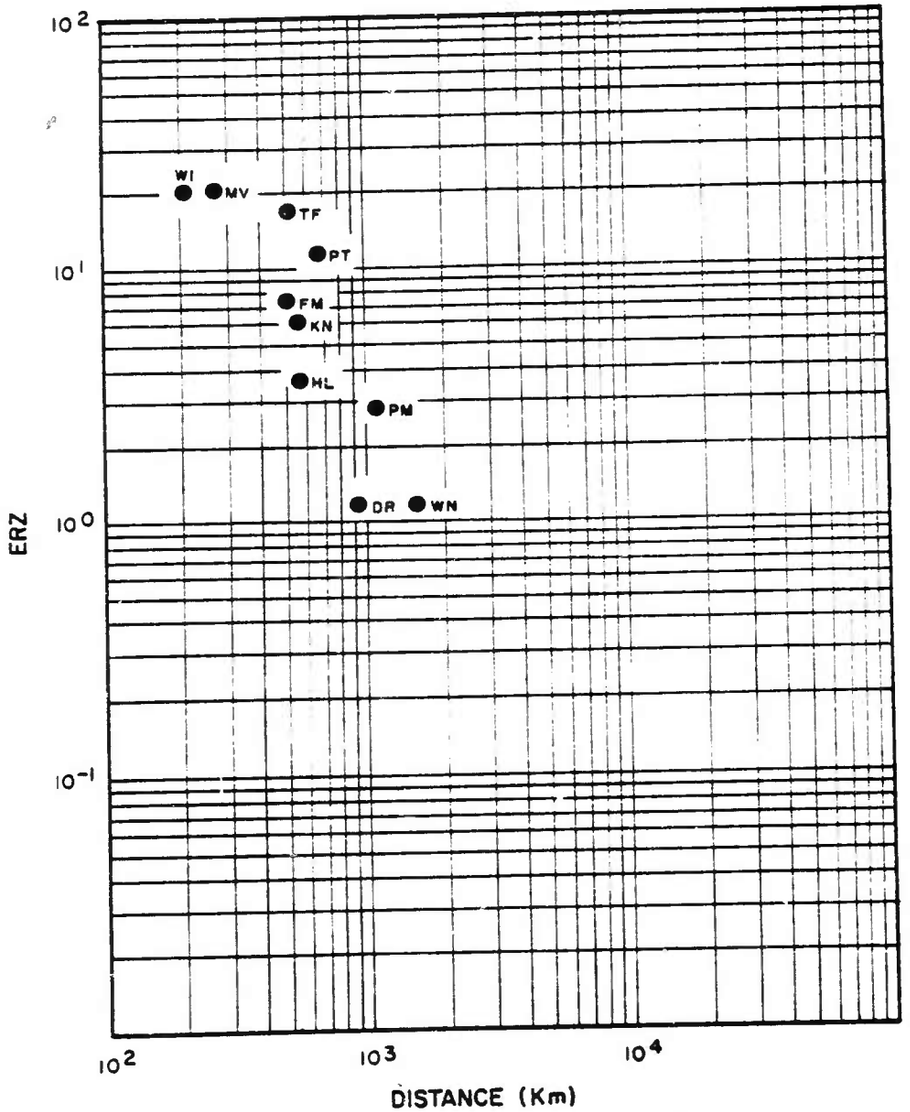

Figure 2c. Fallon Eq. - ERZ vs. Distance.

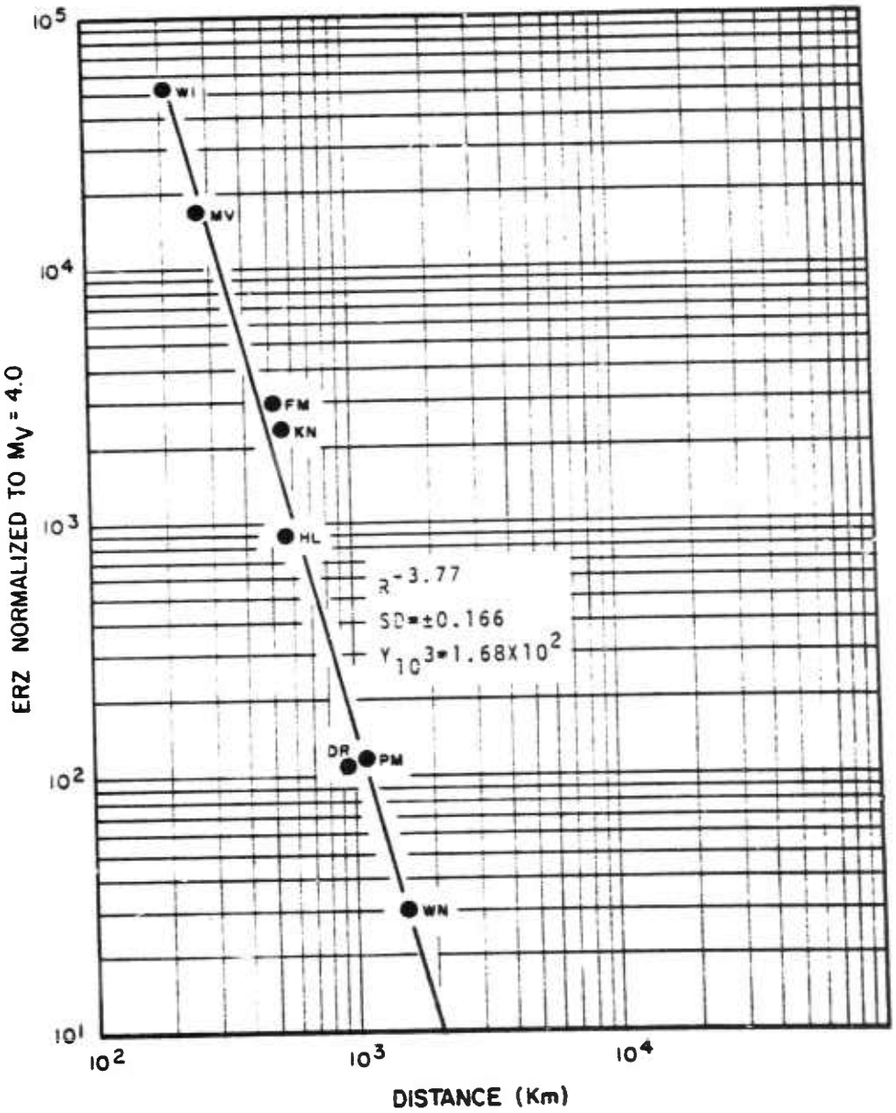

Figure 2d. Fallon Eq. - ERZ vs. Distance. Normalized to surface wave magnitude M_V = 4.0.

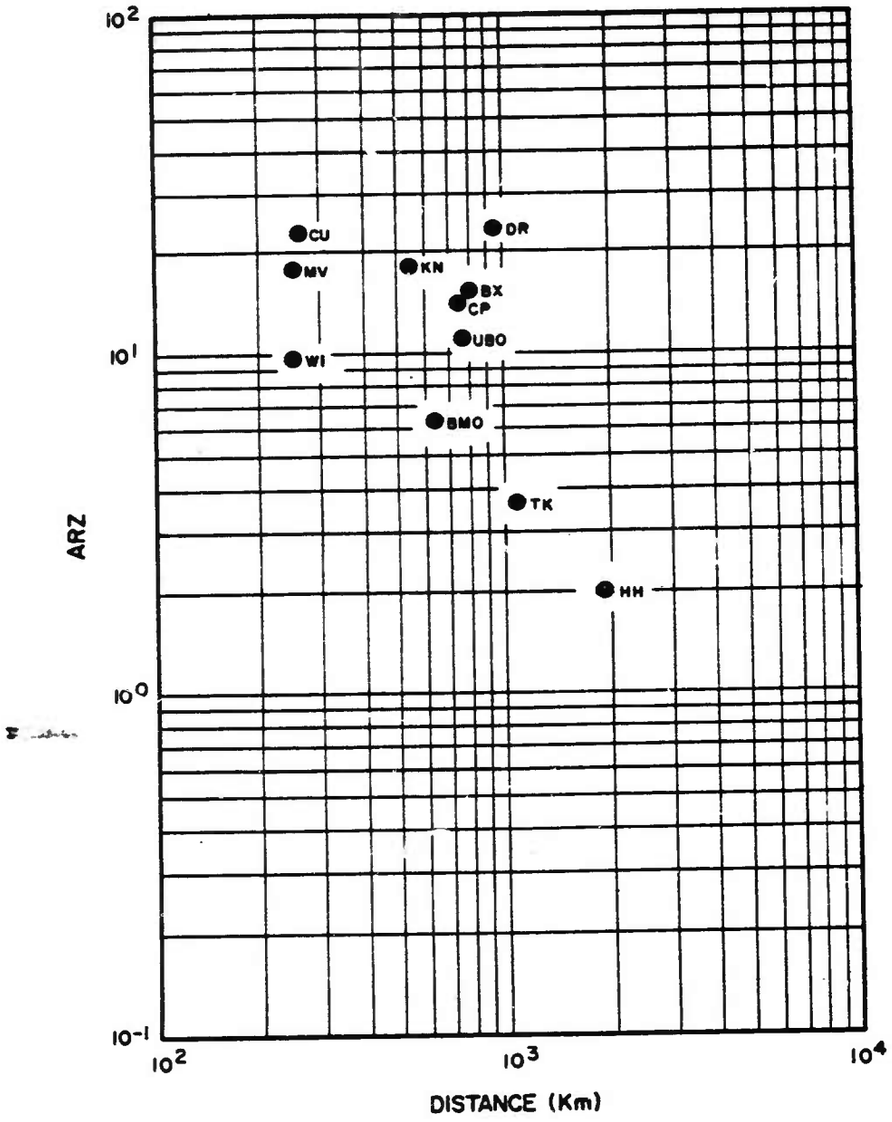

Figure 3a. Shoal - ARZ vs. Distance.

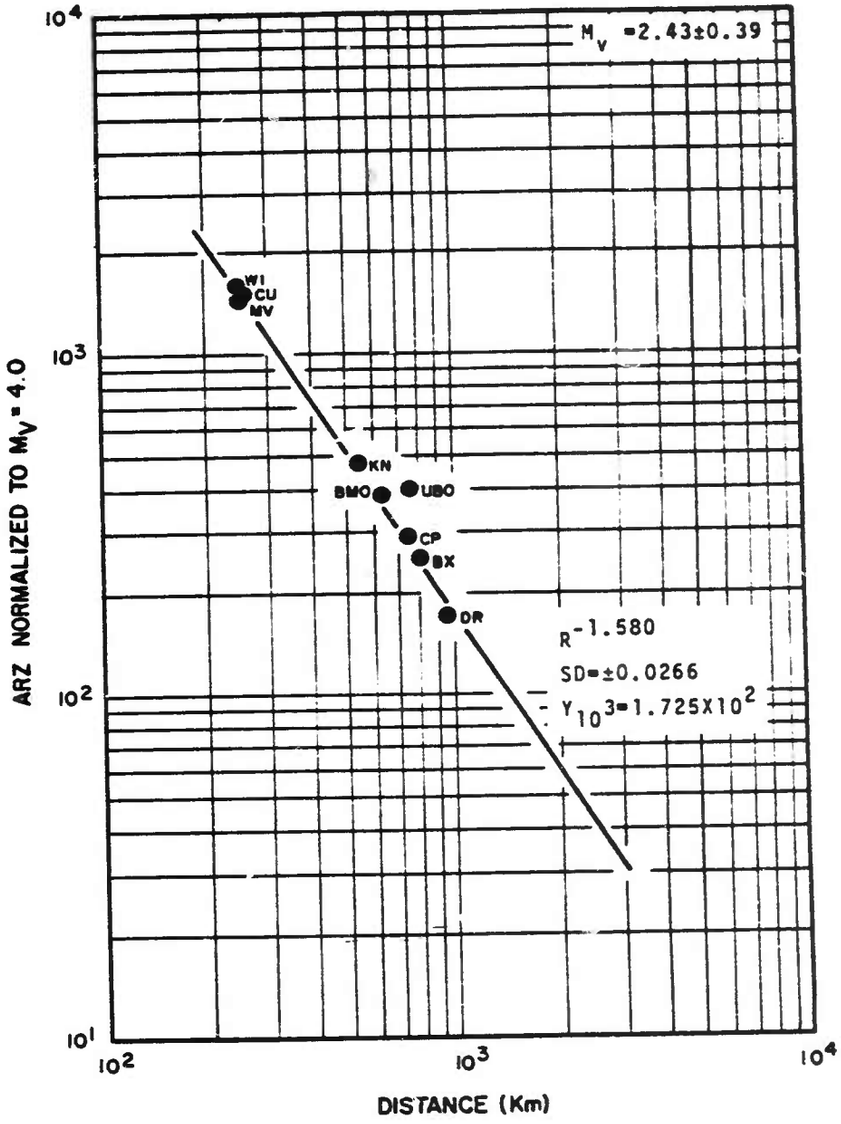

Figure 3b. Shoal - ARZ vs. Distance. Normalized to surface wave magnitude M_V = 4.0.

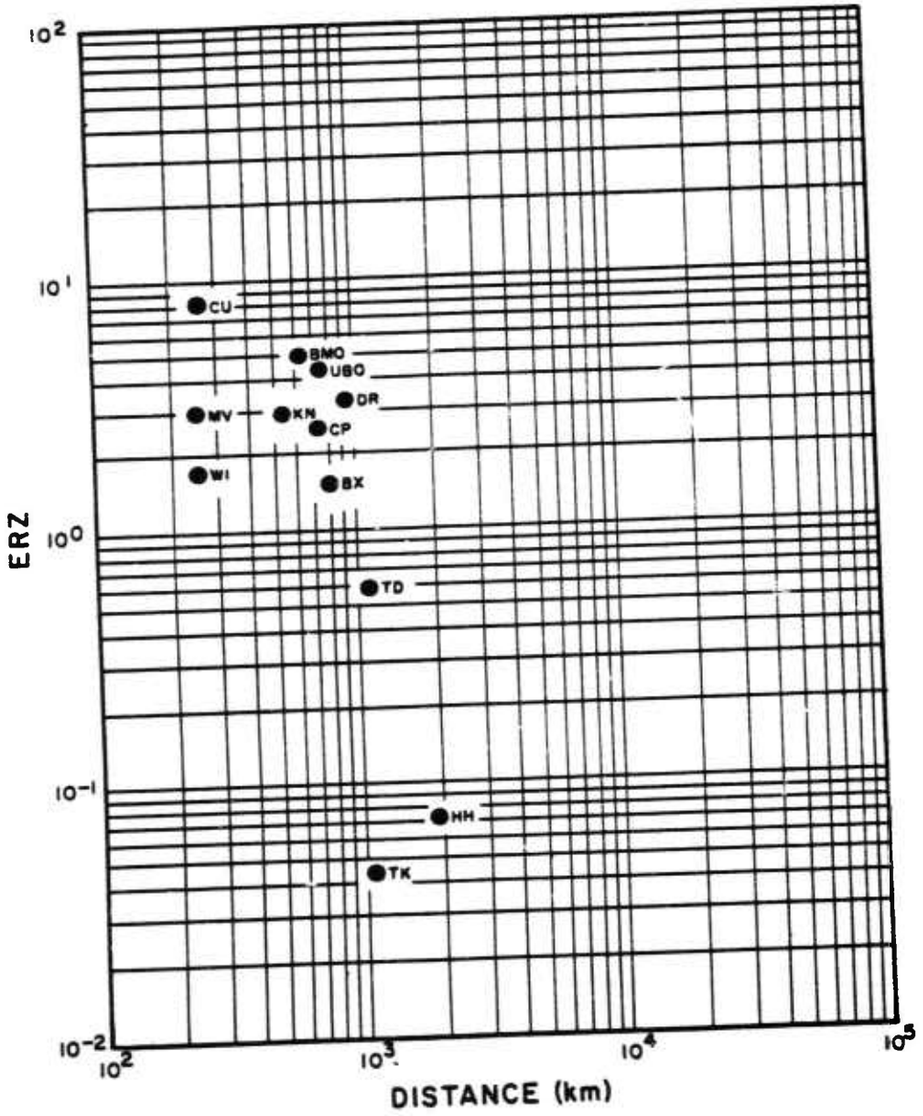

Figure 3c. Shoal - ERZ vs. Distance.

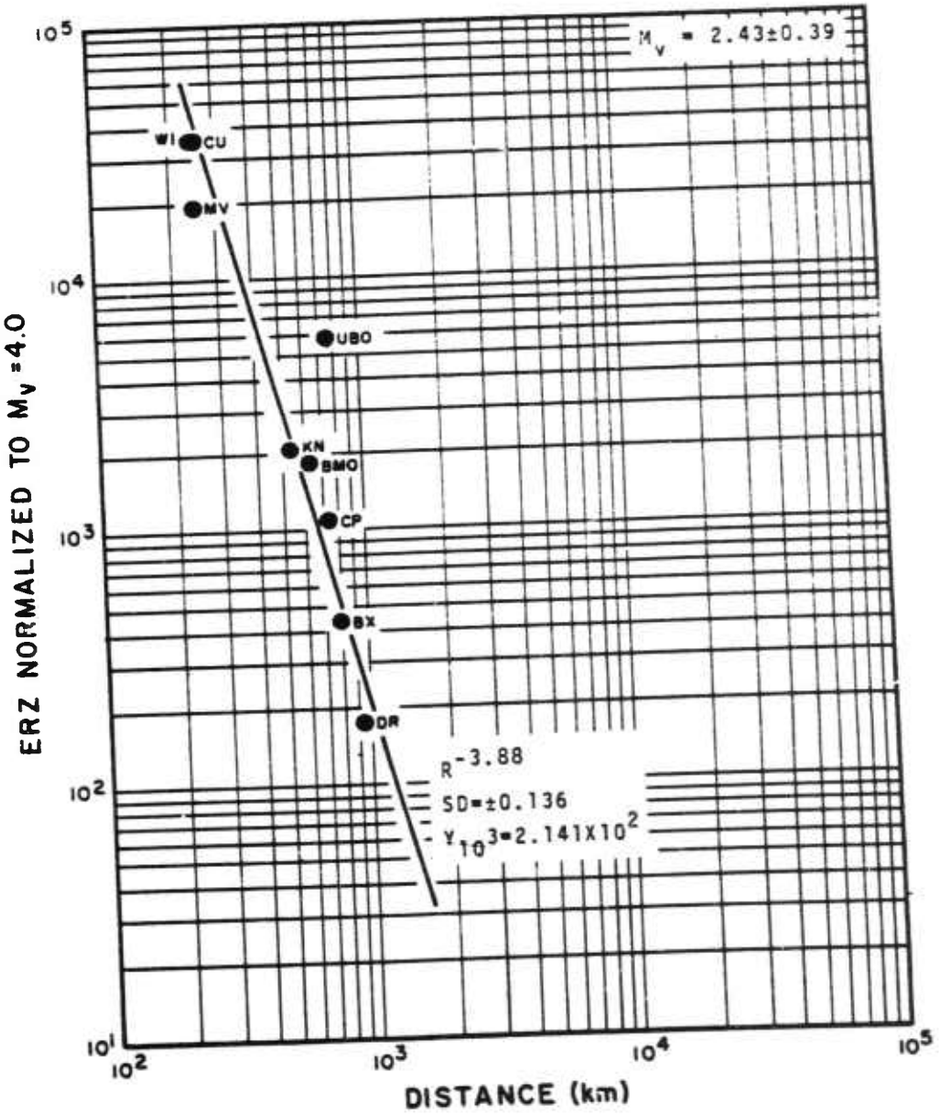

Figure 3d. Shoal - ERZ vs. Distance. Normalized to surface wave magnitude M_v = 4.0.

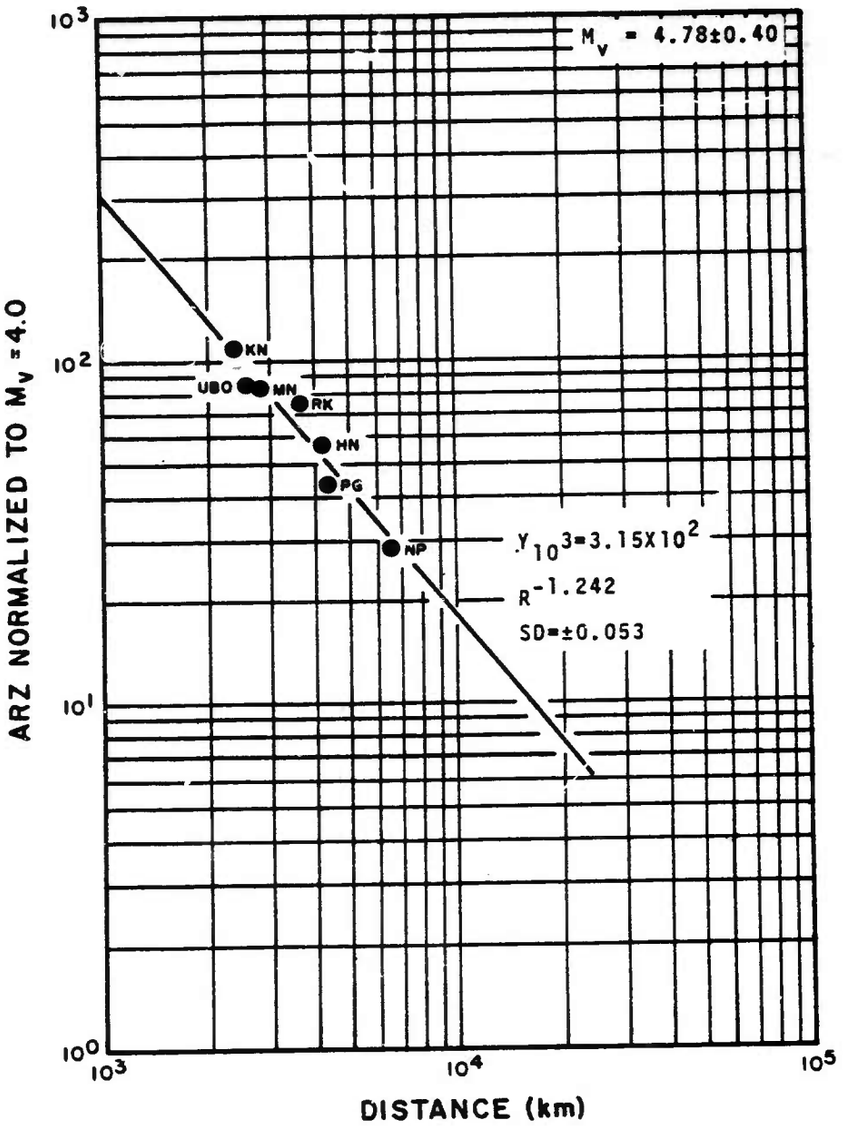

Figure 4a. Guerrero, Mexico Eq. - ARZ vs. Distance. Normalized to surface wave magnitude M_v = 4.0.

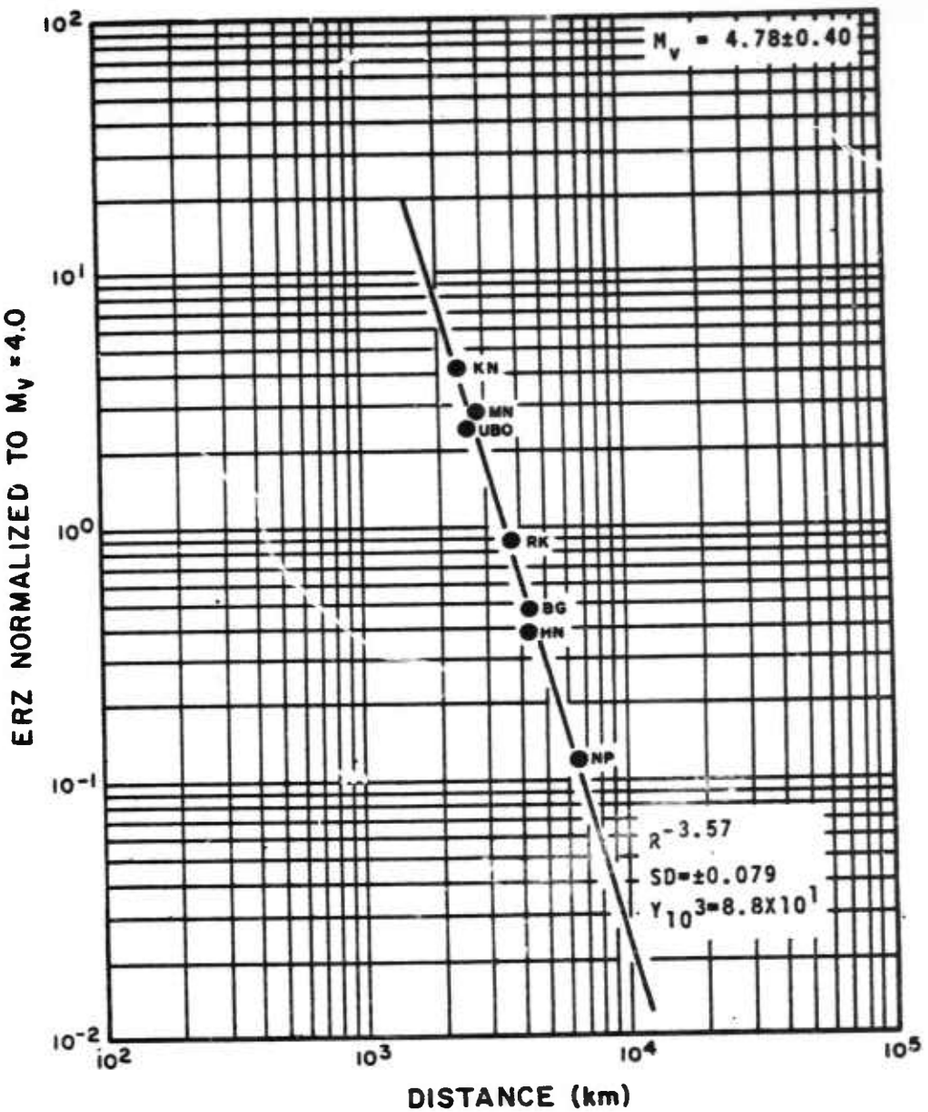

Figure 4b. Guerrero, Mexico Eq. - ERZ vs. Distance. Normalized to surface wave magnitude M_v = 4.0.

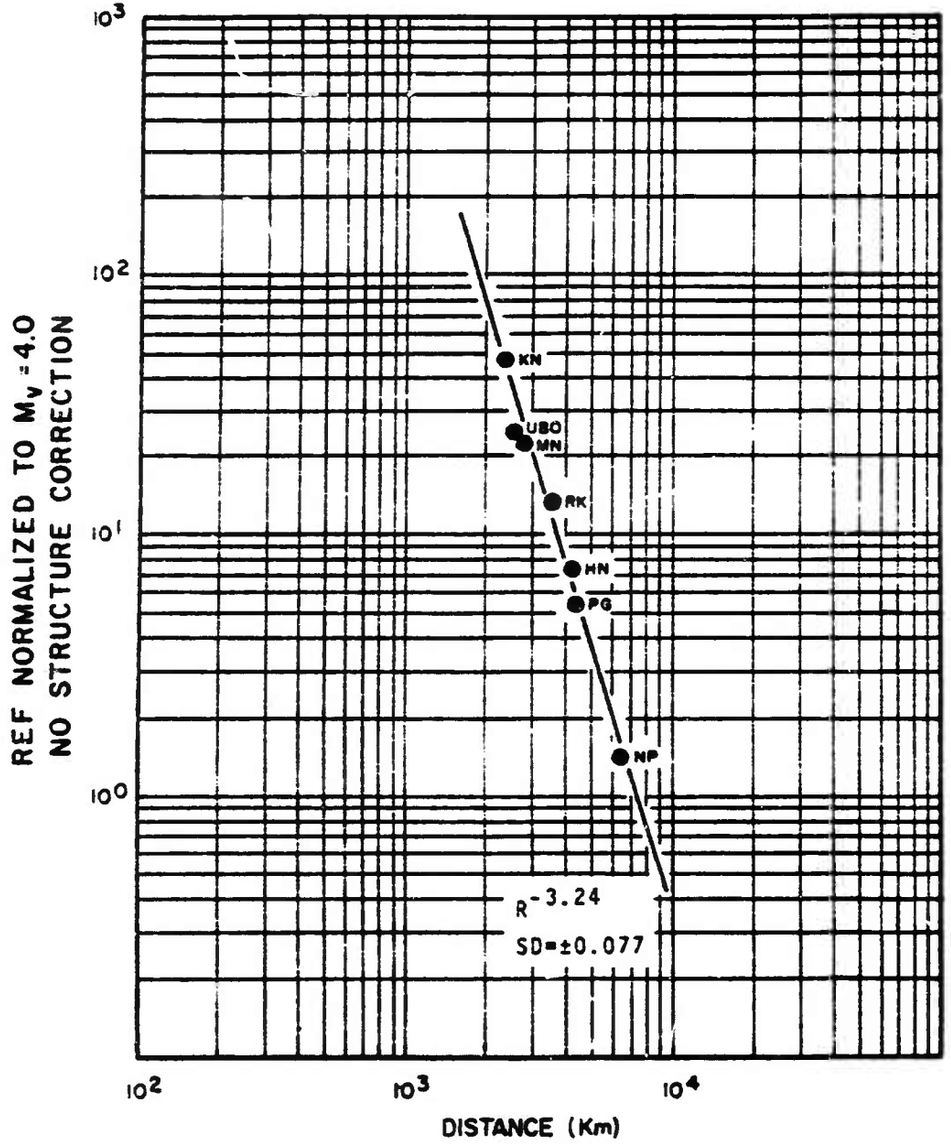

Figure 4c. Guerrero, Mexico Eq - REF vs. Distance. No structure correction. Normalized to surface wave magnitude M_V = 4.0.

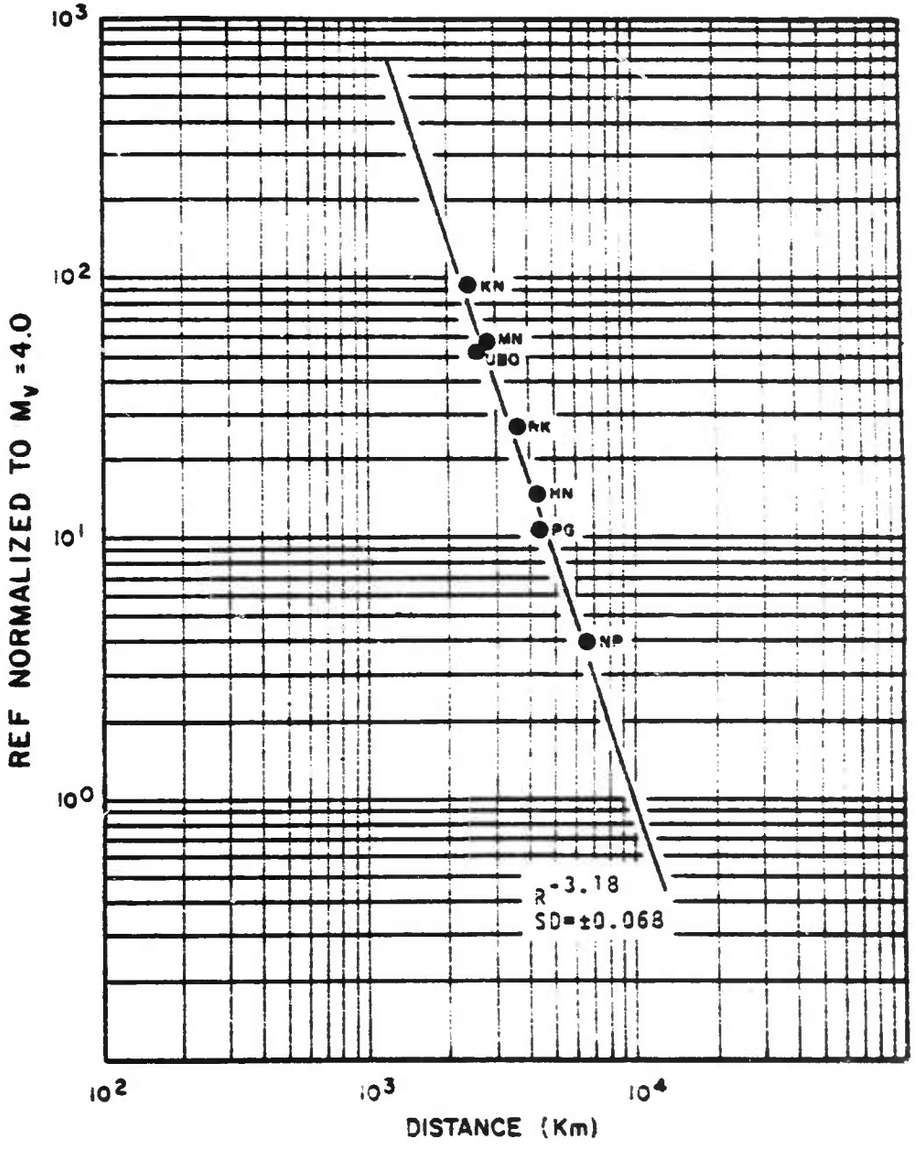

Figure 4d. Guerrero, Mexico Eq - REF vs. Distance. Structure correction. Normalized to surface wave magnitude M_V = 4.0.

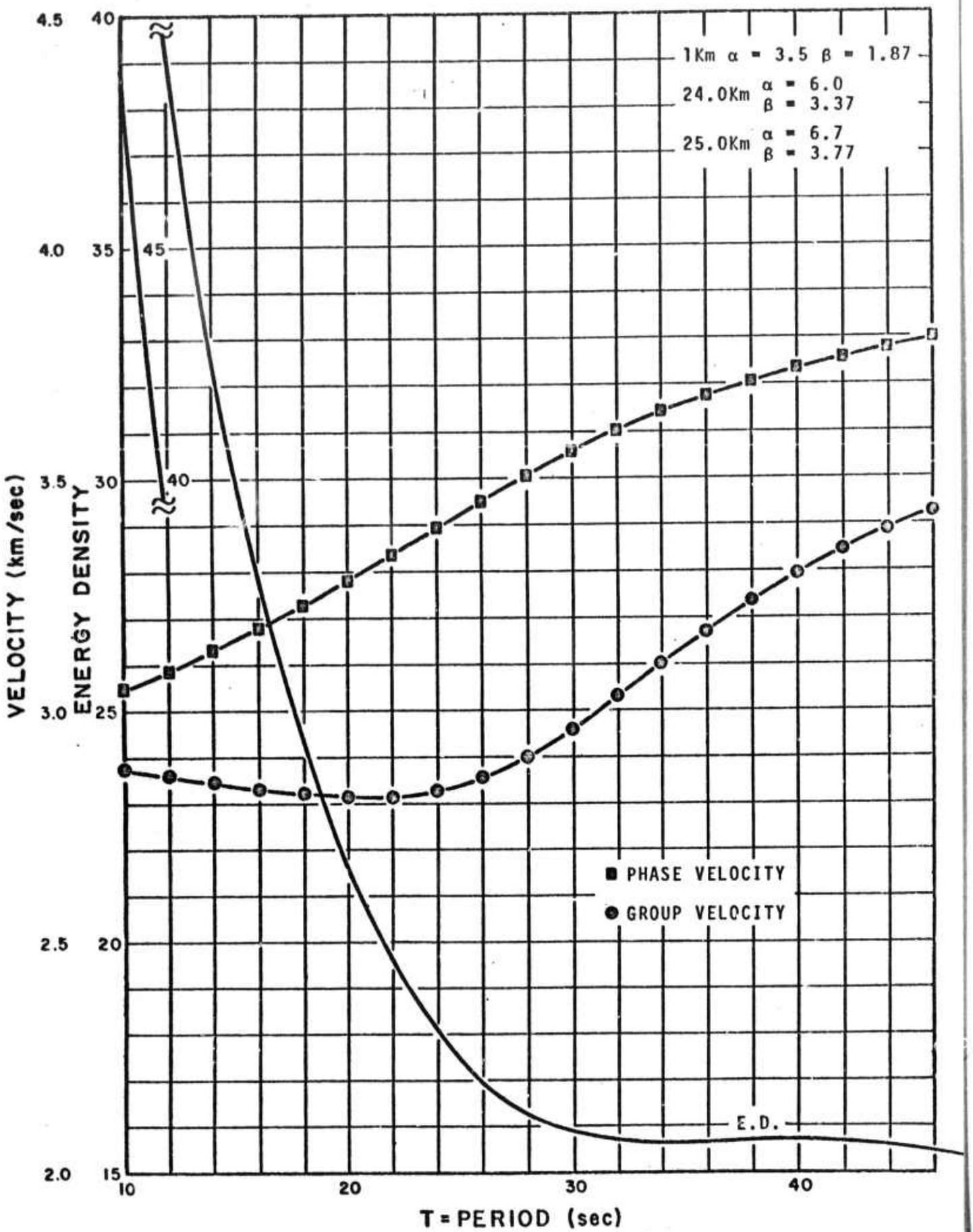

Figure 4e. Energy Density vs. Period at FK-CO.

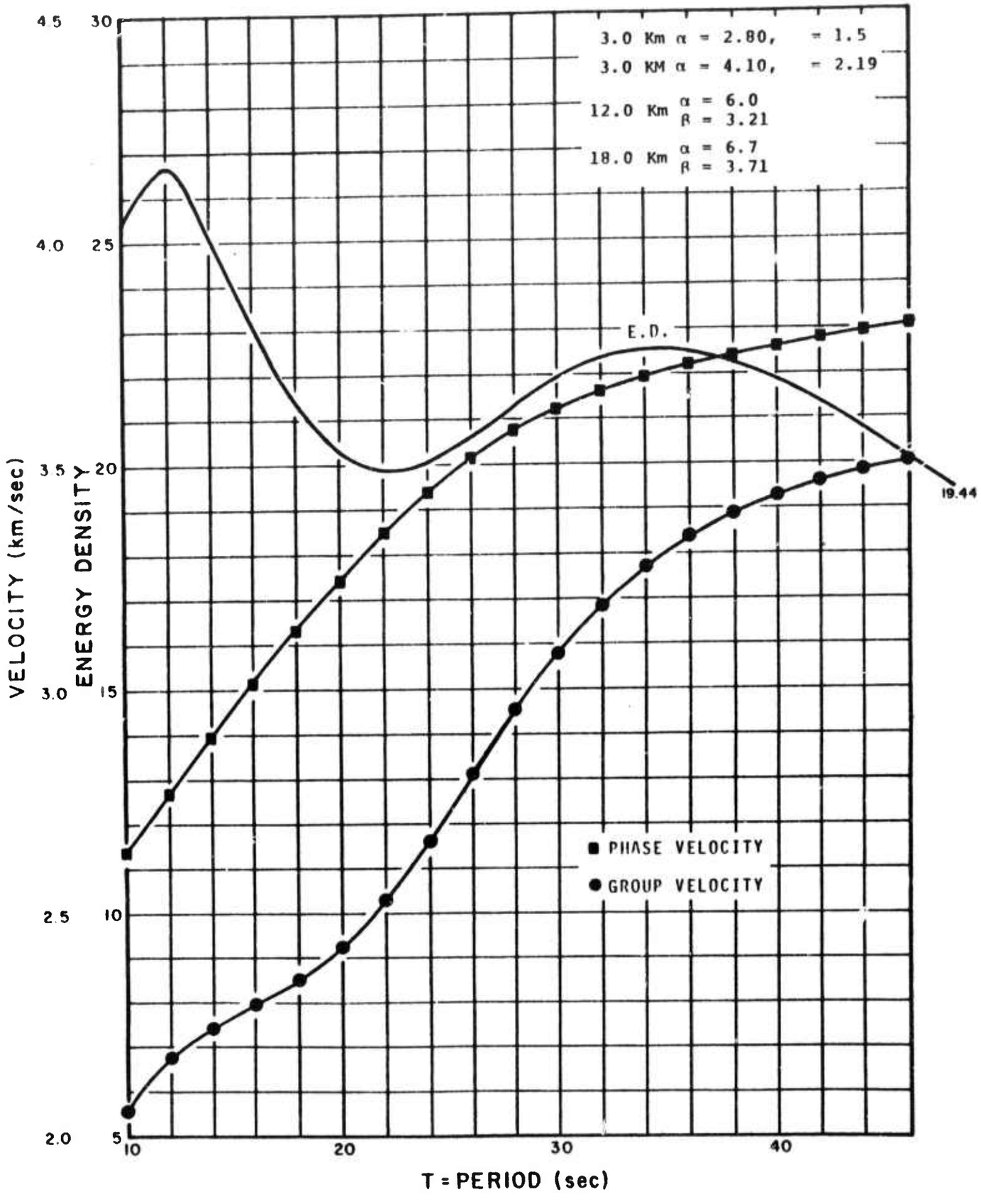

Figure 4f. Energy Density vs. Period at UBO.

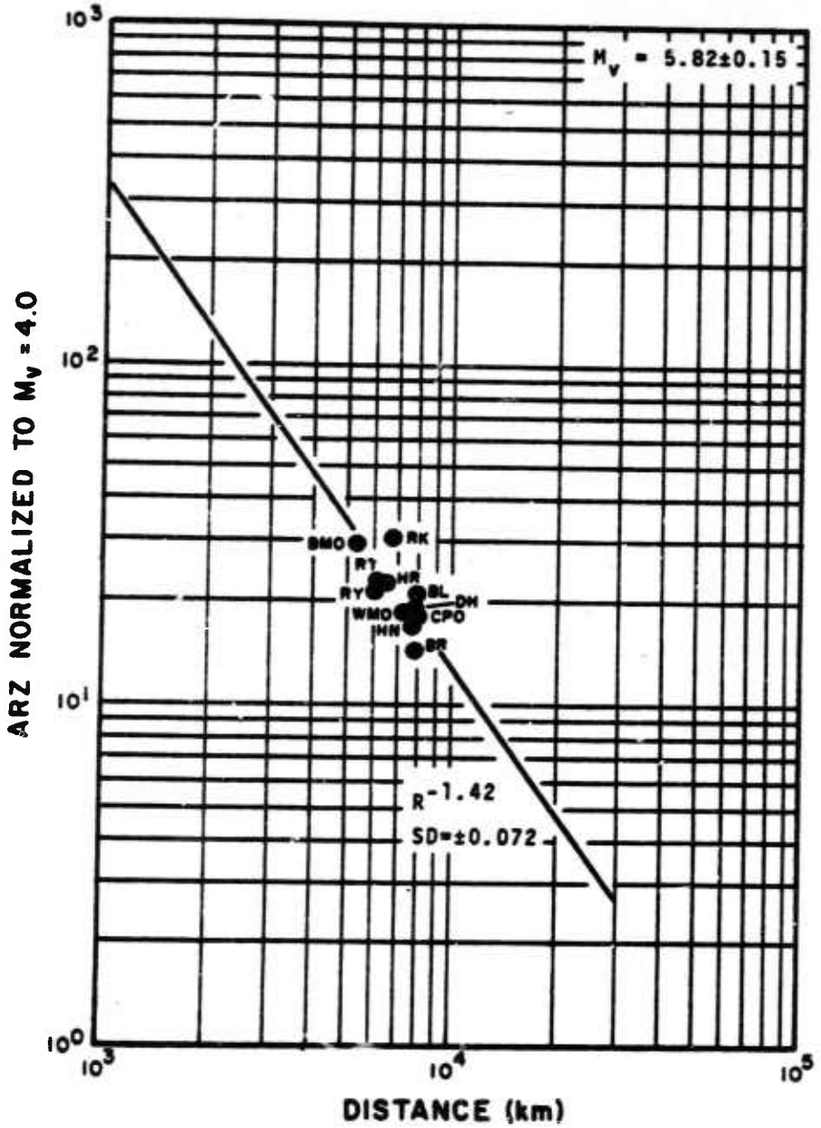

Figure 5a. Komandorsky Islands Eq I - ARZ vs. Distance. Normalized to surface wave magnitude M_v = 4.0.

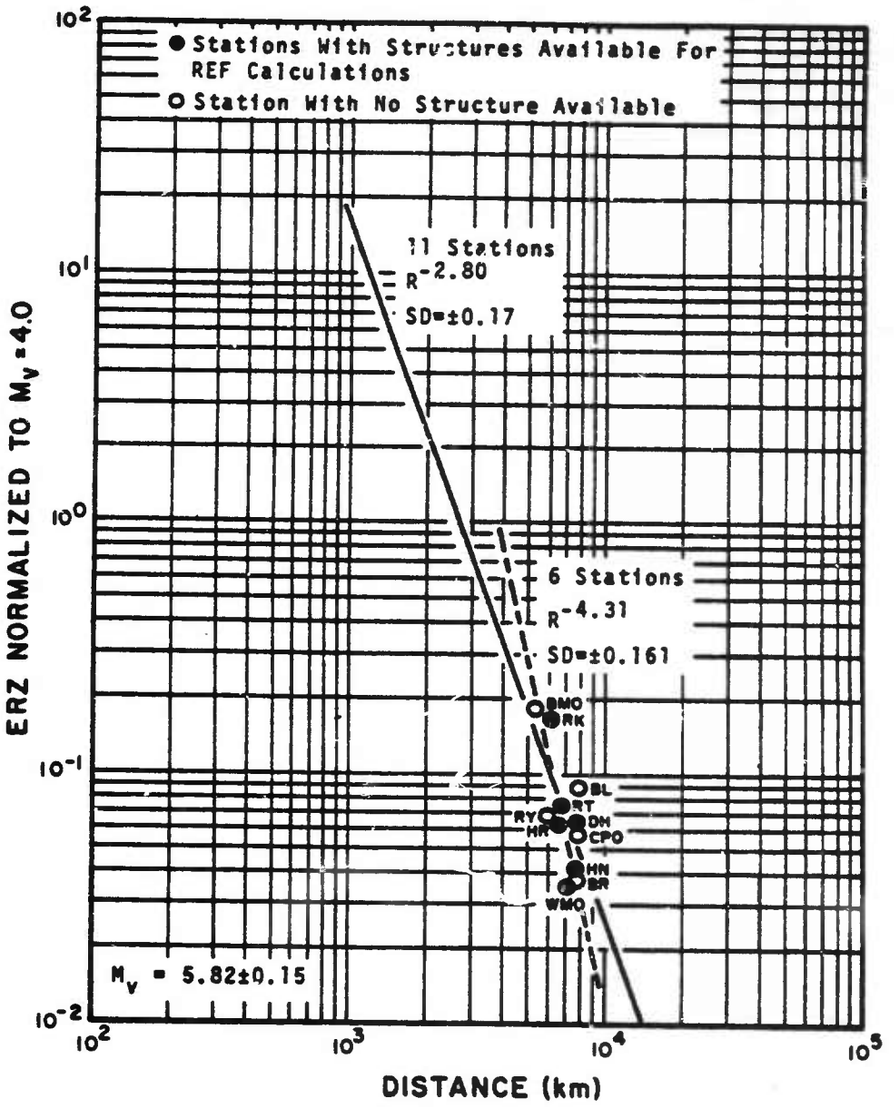

Figure 5b. Komandorsky Islands Eq I - ERZ vs. Distance. Normalized to surface wave magnitude M_v = 4.0.

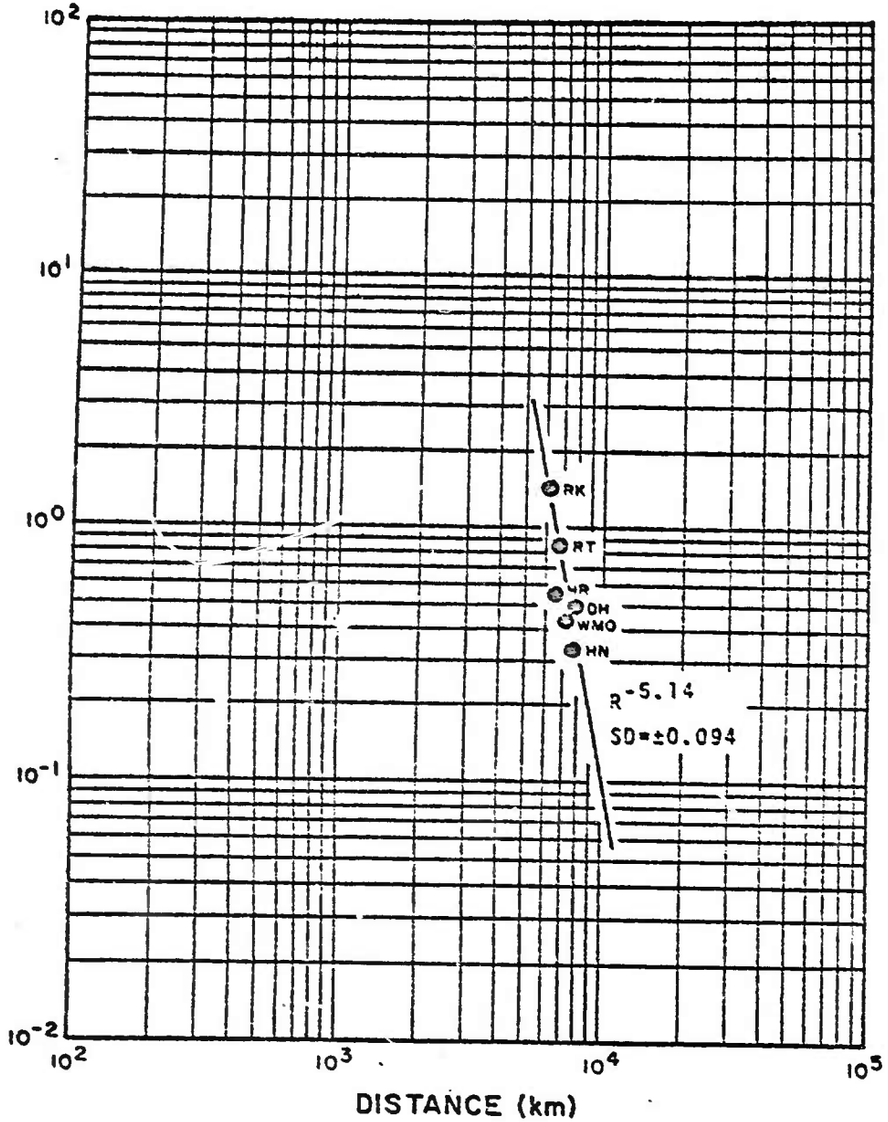

Figure 5c. Komandorsky Islands Eq I - REF vs. Distance. No structure correction. Normalized to surface wave magnitude M_v = 4.0.

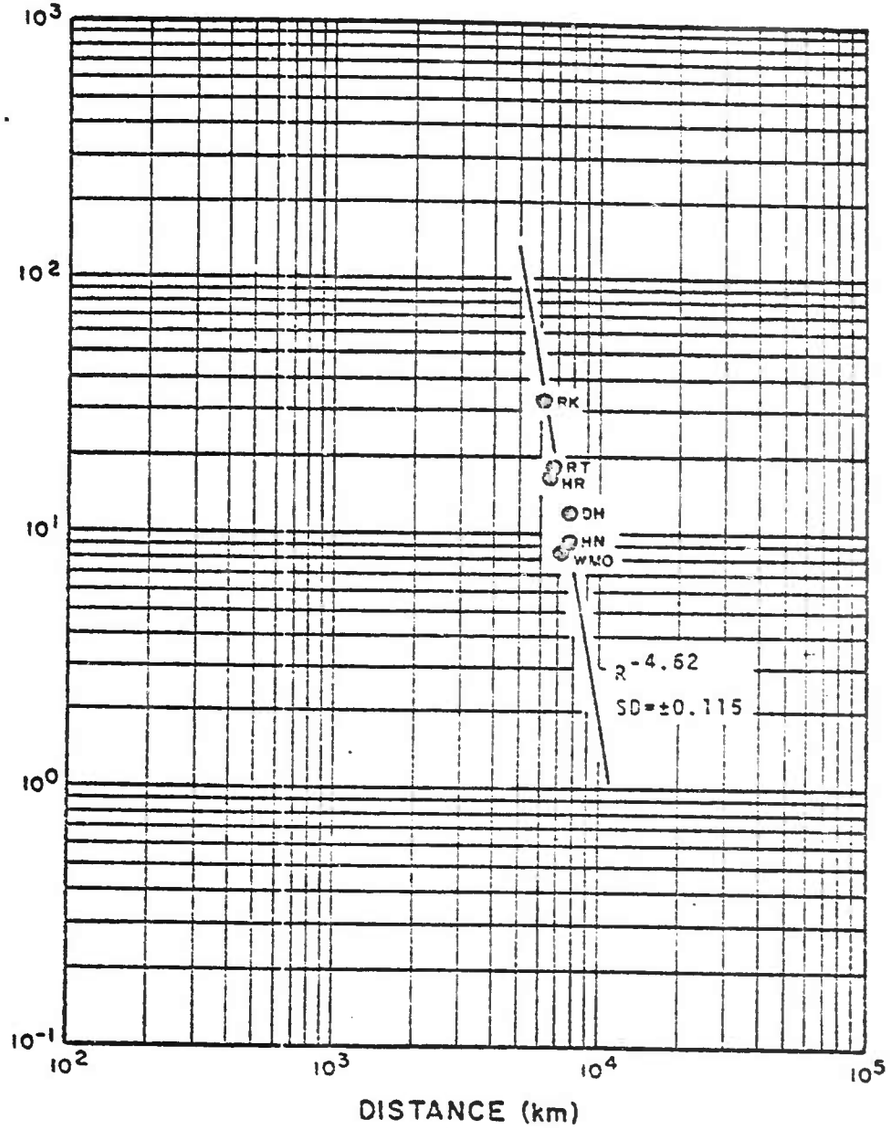

Figure 5d. Komandorsky Islands Eq I - REF vs. Distance. Structure correction. Normalized to surface wave magnitude M_v = 4.0.

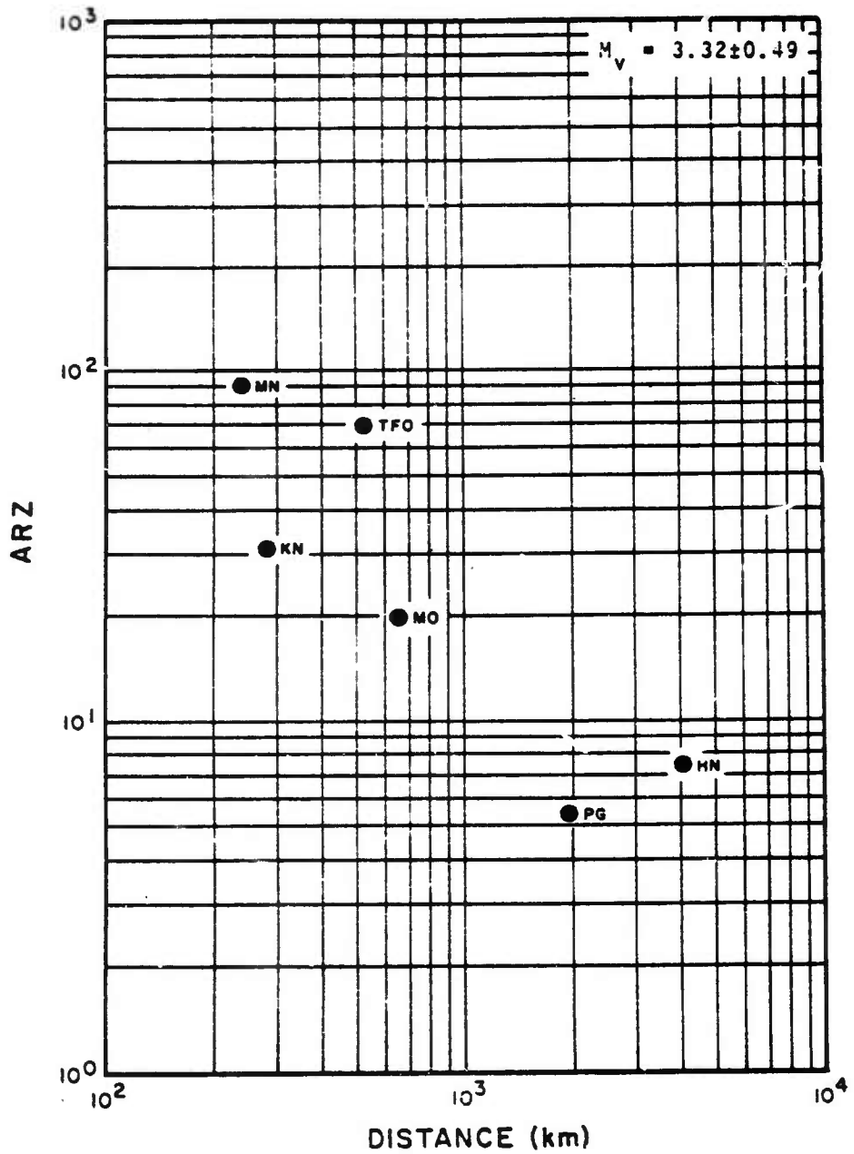

Figure 6a. Bourbon - ARZ vs. Distance.

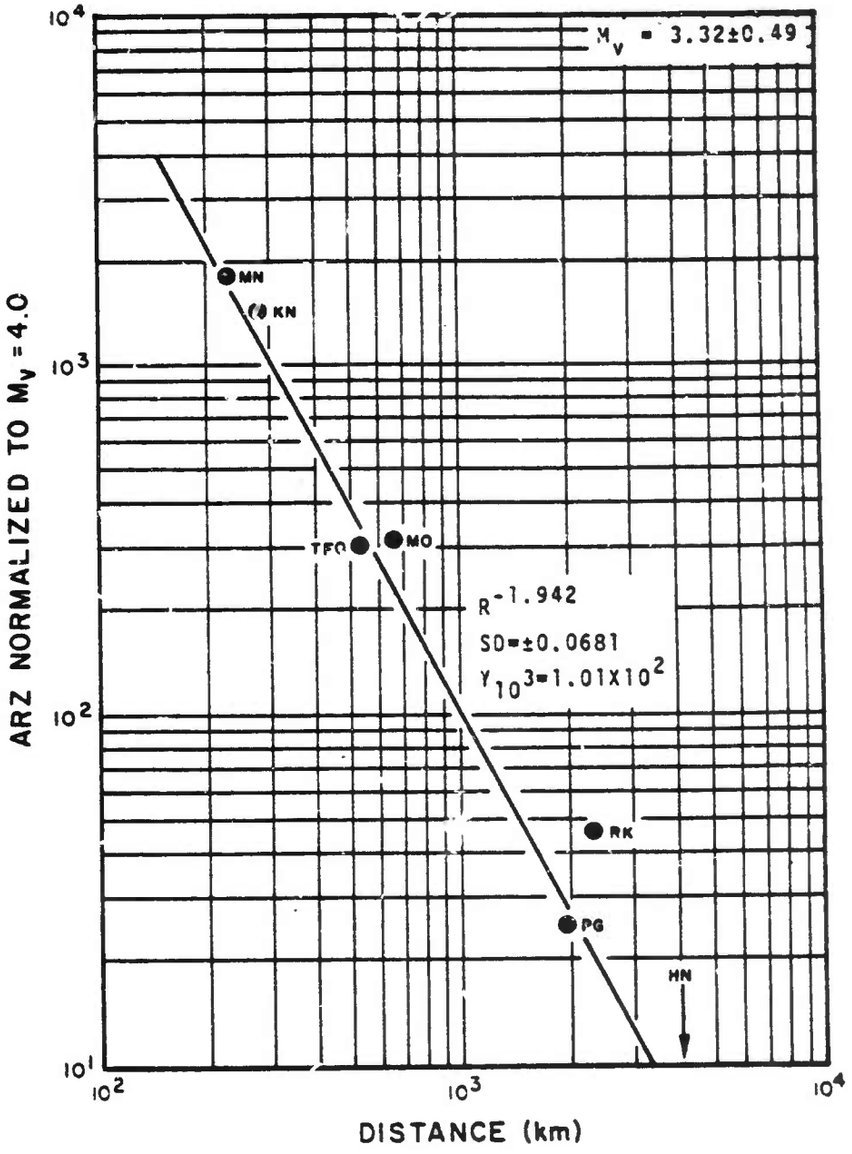

Figure 6b. Bourbon - ARZ vs. Distance. Normalized to surface wave magnitude M_v = 4.0.

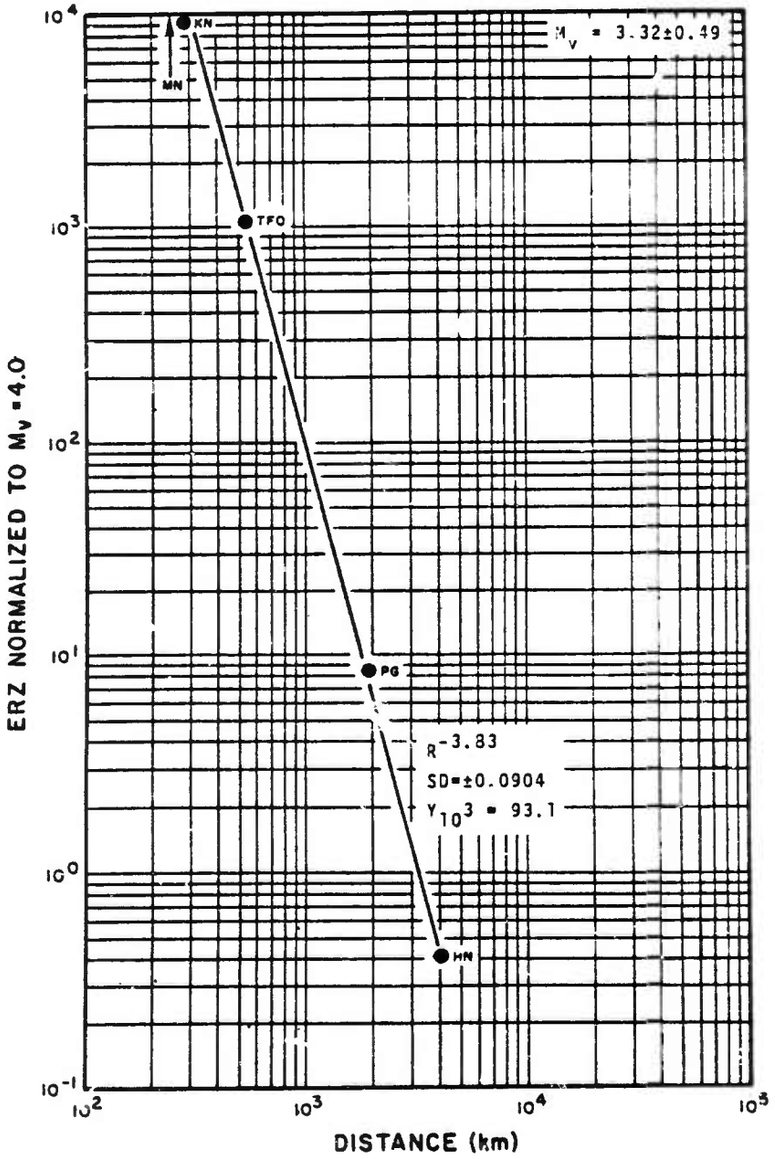

Figure 6c. Bourbon - ERZ vs. Distance. Normalized to surface wave magnitude M_v = 4.0.

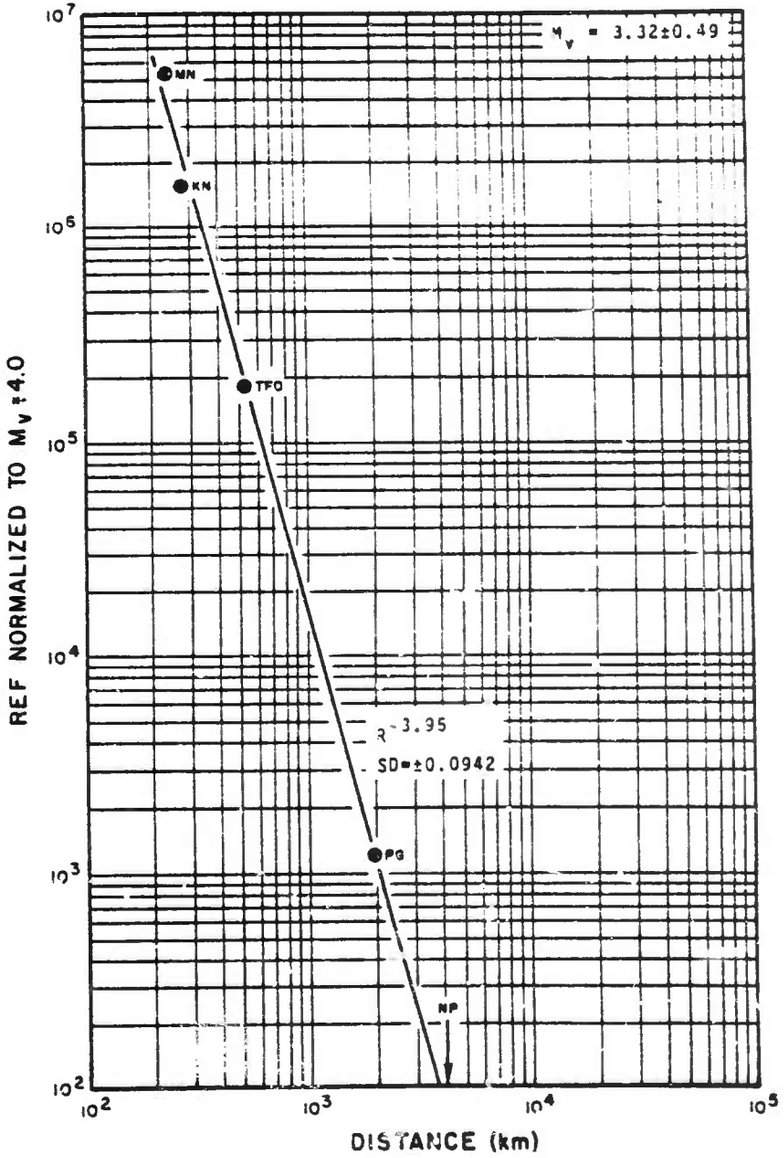

Figure 6d. Bourbon - REF vs. Distance. Structure correction. Normalized to surface wave magnitude M_v = 4.0.

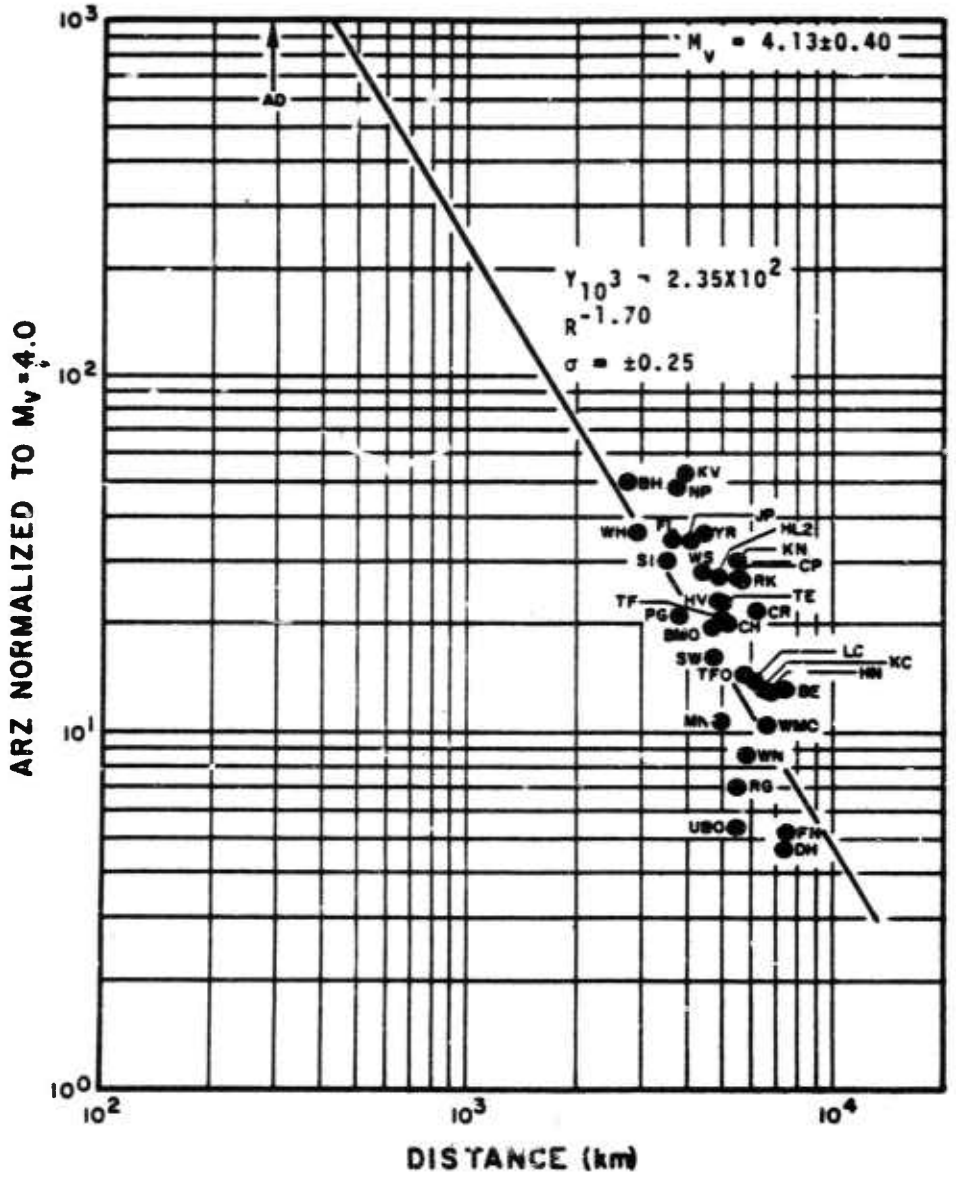

Figure 7a. Long Shot - ARZ vs. Distance. Normalized to surface wave magnitude M_V = 4.0.

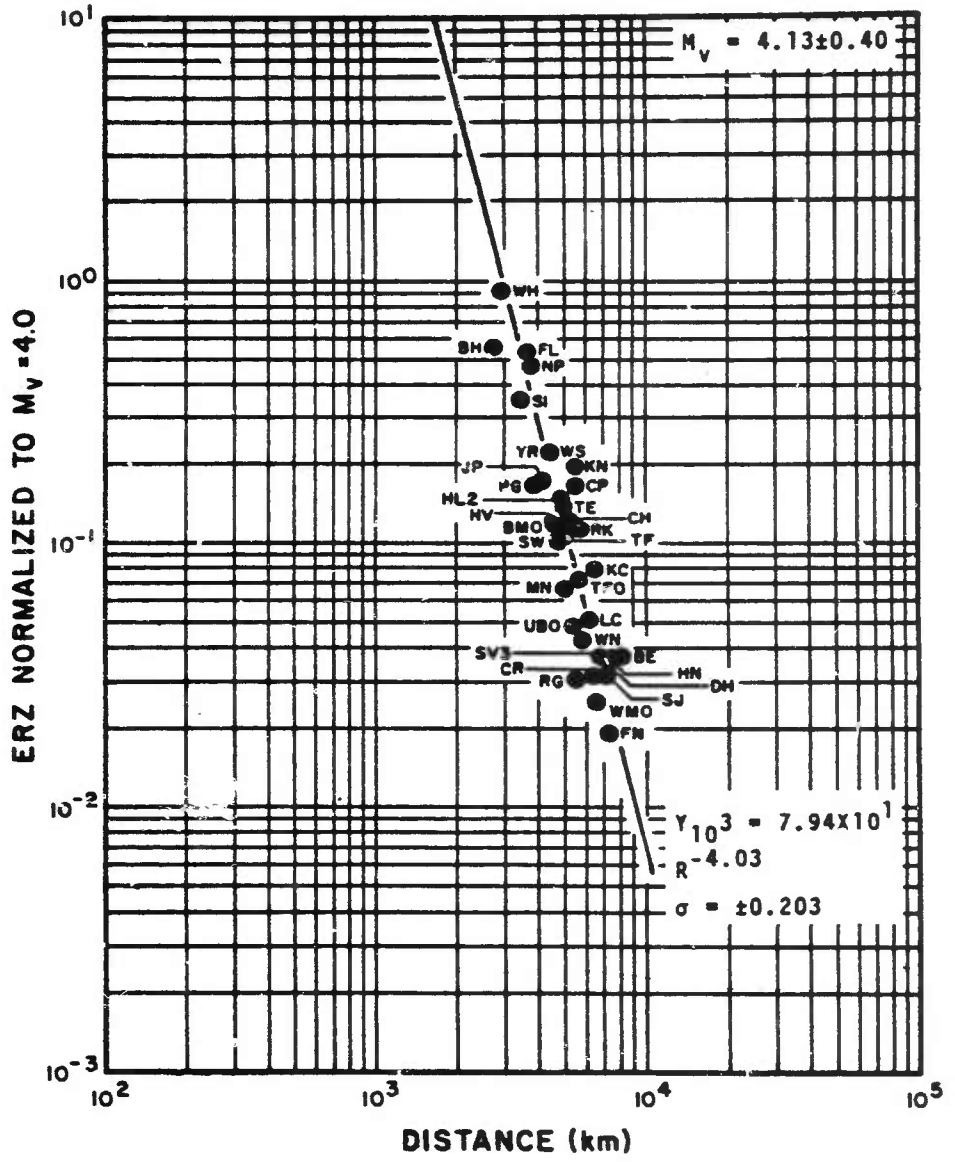

Figure 7b. Long Shot - ERZ vs. Distance. Normalized to surface wave magnitude M_V = 4.0.

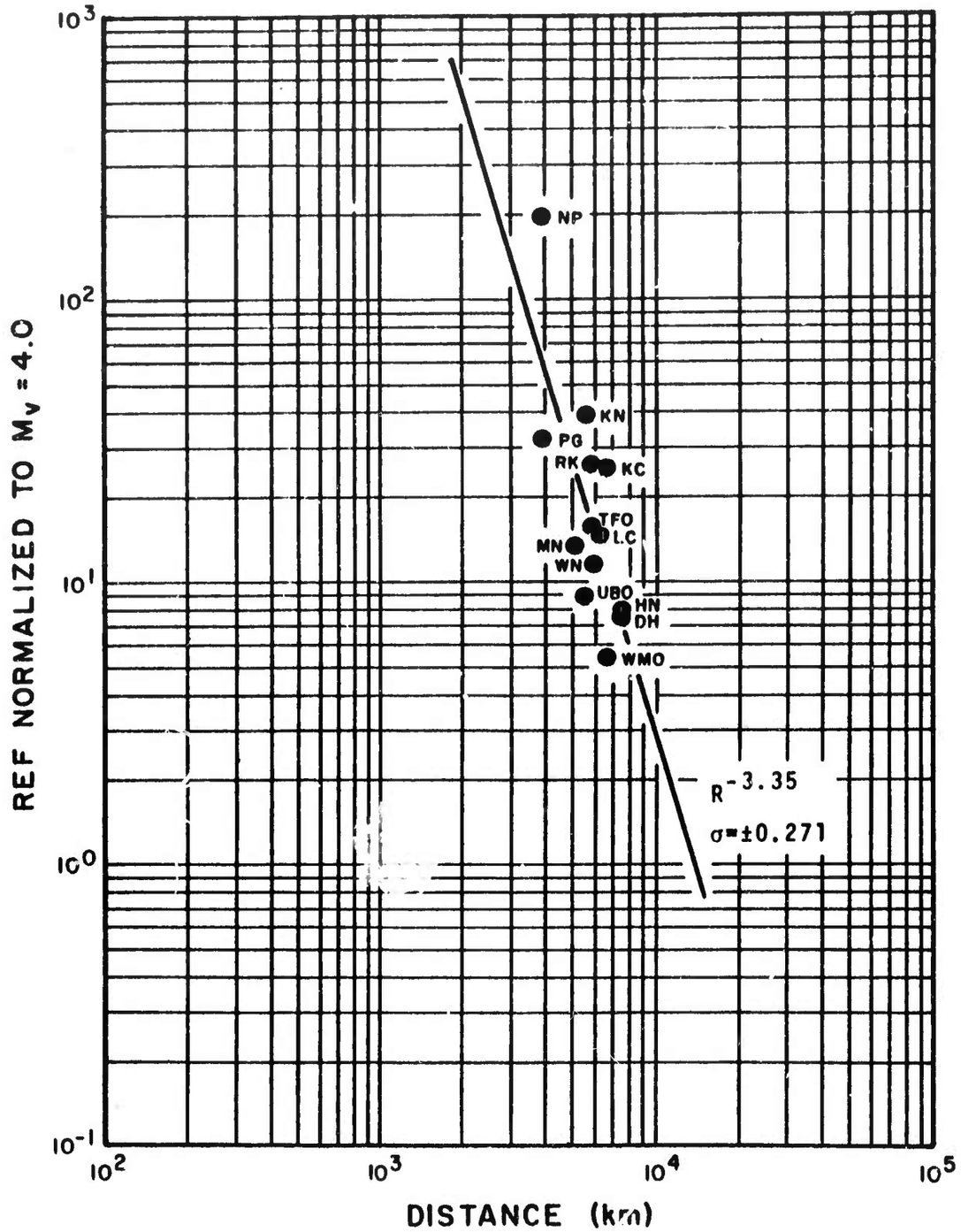

Figure 7c. Long Shot - REF vs. Distance. Structure correction. Normalized to surface wave magnitude $M_V = 4.0$.

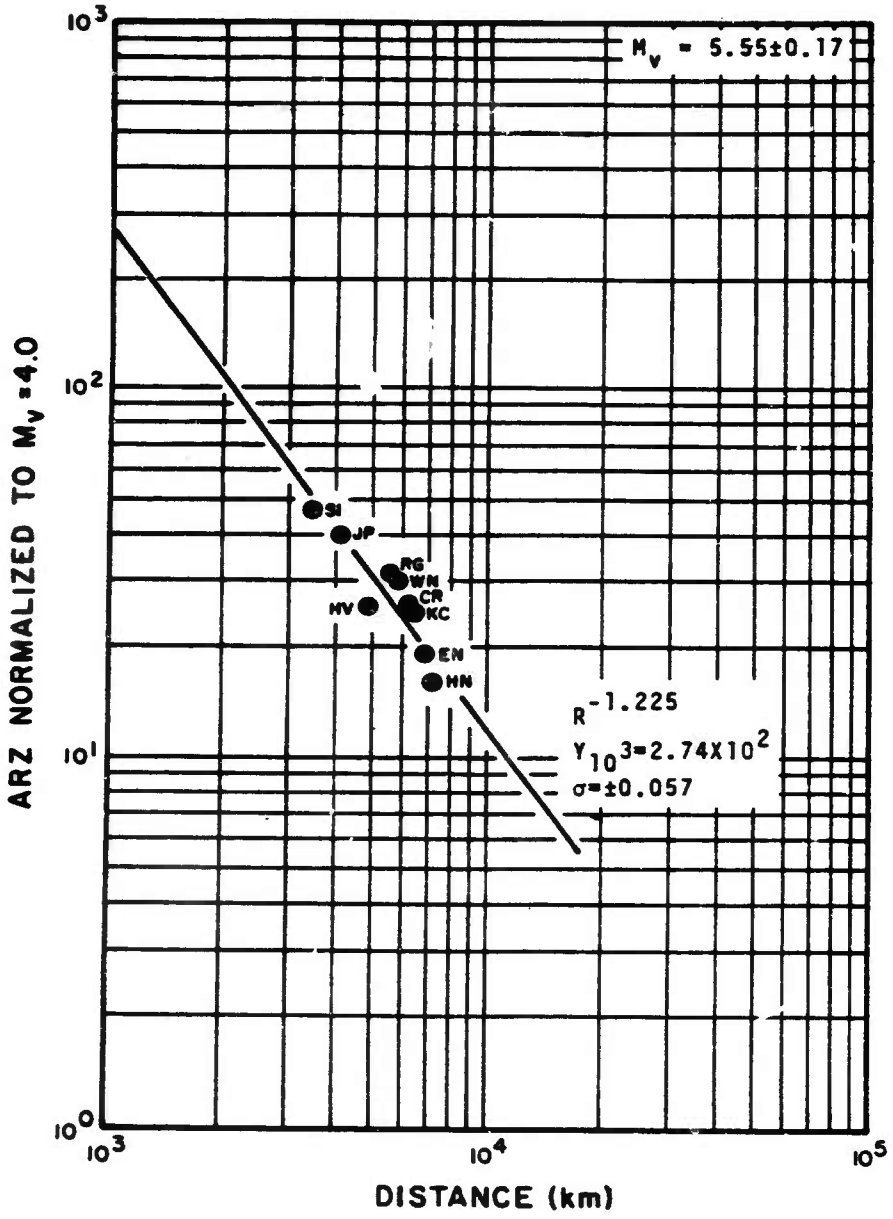

Figure 8a. Andreanof Is. Eq - ARZ vs Distance. Normalized to surface wave magnitude M_v = 4.0.

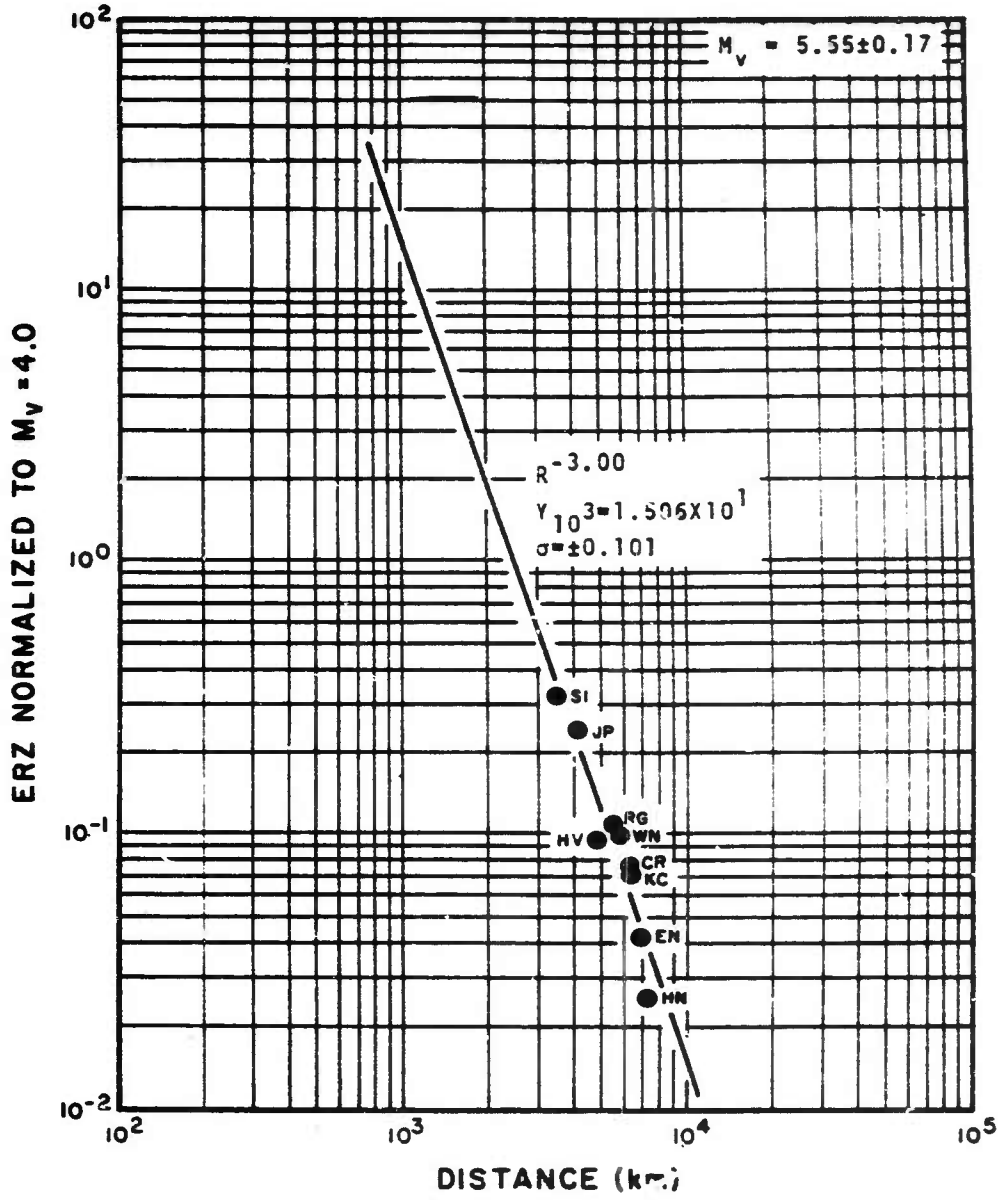

Figure 8b. Andreanof Is. Eq - ERZ vs Distance. Normalized to surface wave magnitude M_v = 4.0.

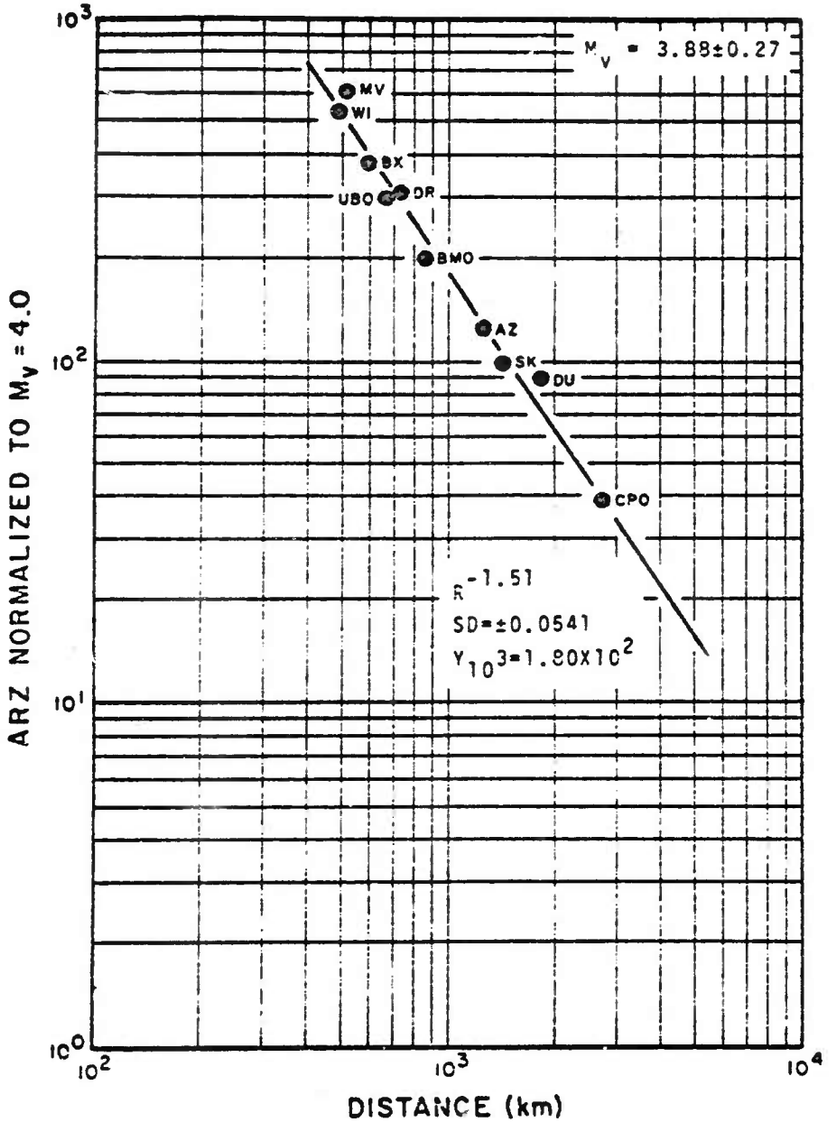

Figure 9a. Bilby - ARZ vs. Distance-Normalized to surface wave magnitude M_V = 4.0.

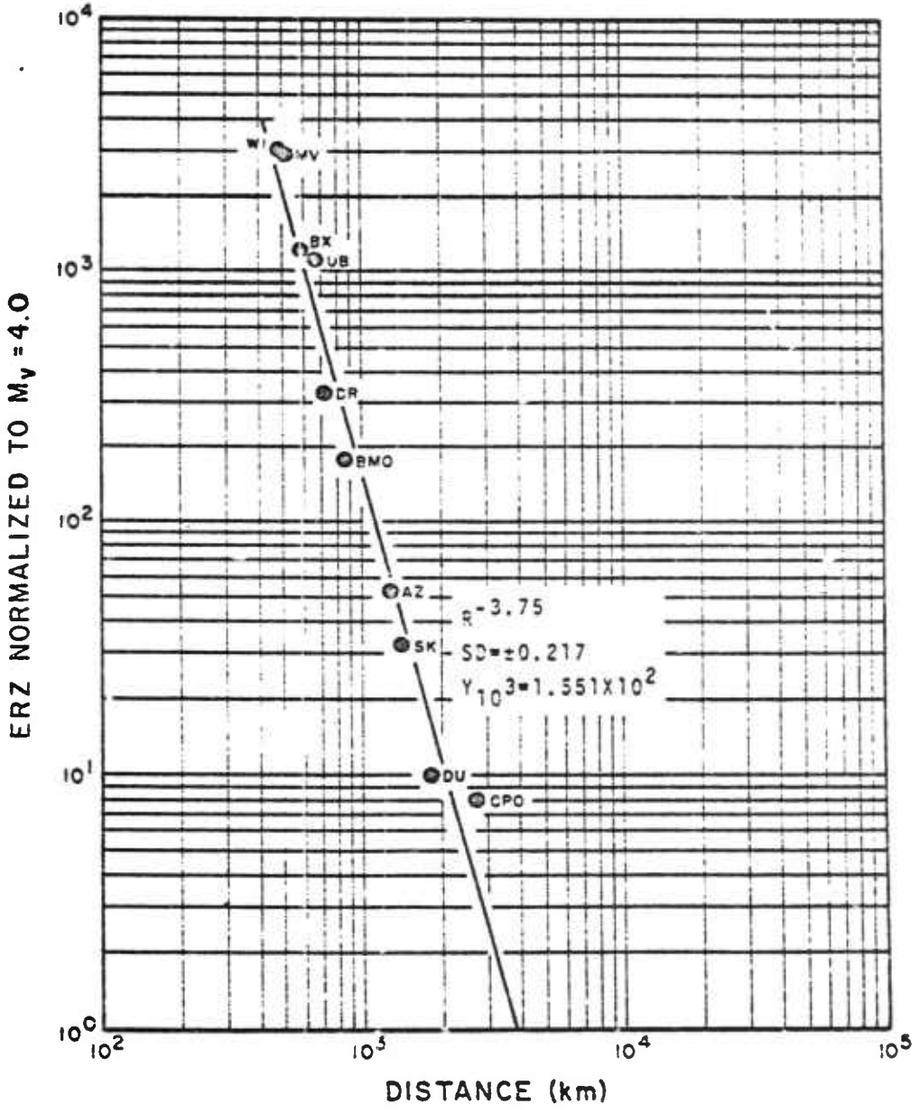

Figure 9b. Bilby - ERZ vs. Distance-Normalized to surface wave magnitude M_V - 4.0.

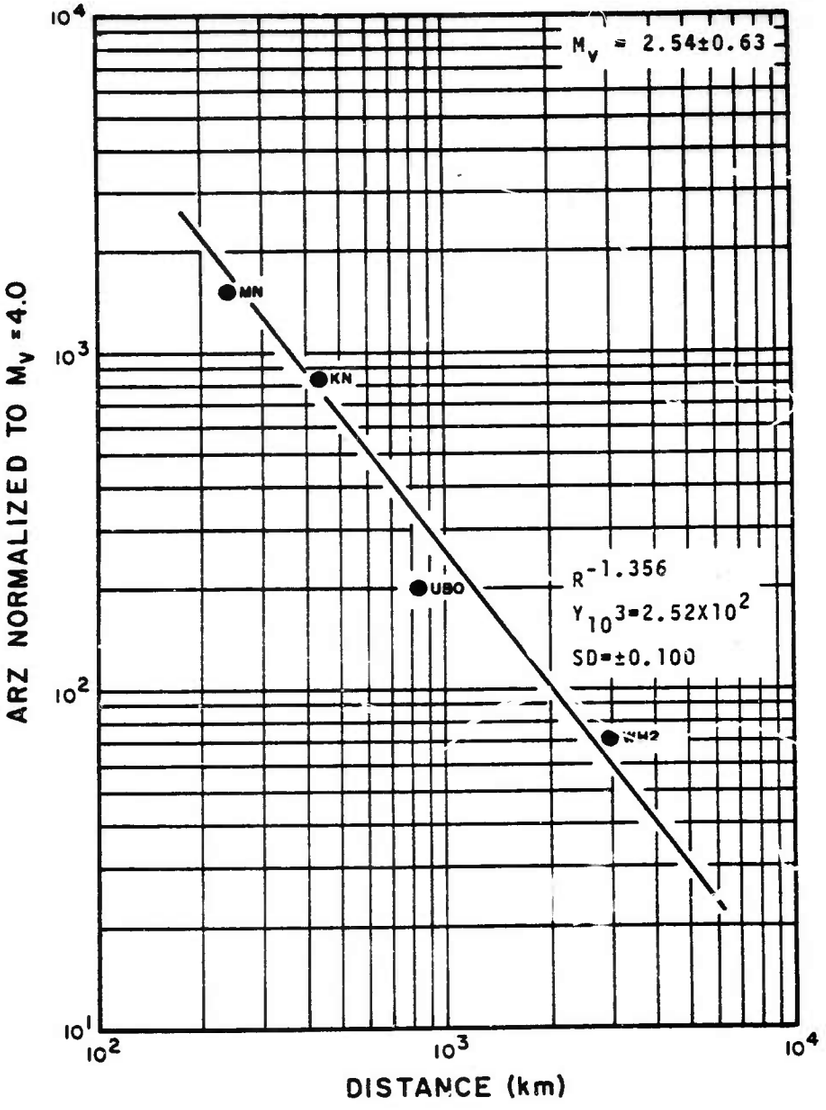

Figure 10a. Calif-Nevada Border Eq - ARZ vs. Distance. Normalized to surface wave magnitude M_v = 4.0.

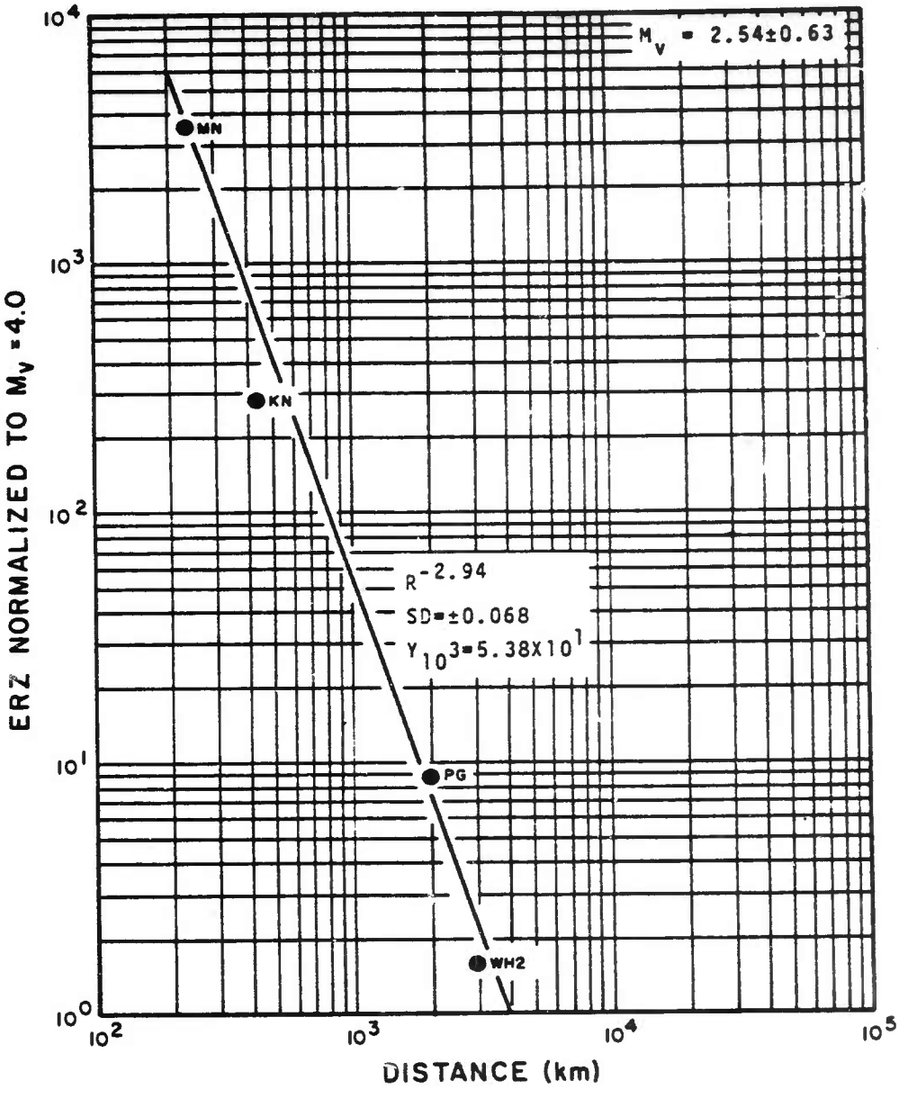

Figure 10b. Calif-Nevada Border Eq - ERZ vs. Distance. Normalized to surface wave magnitude M_v = 4.0.

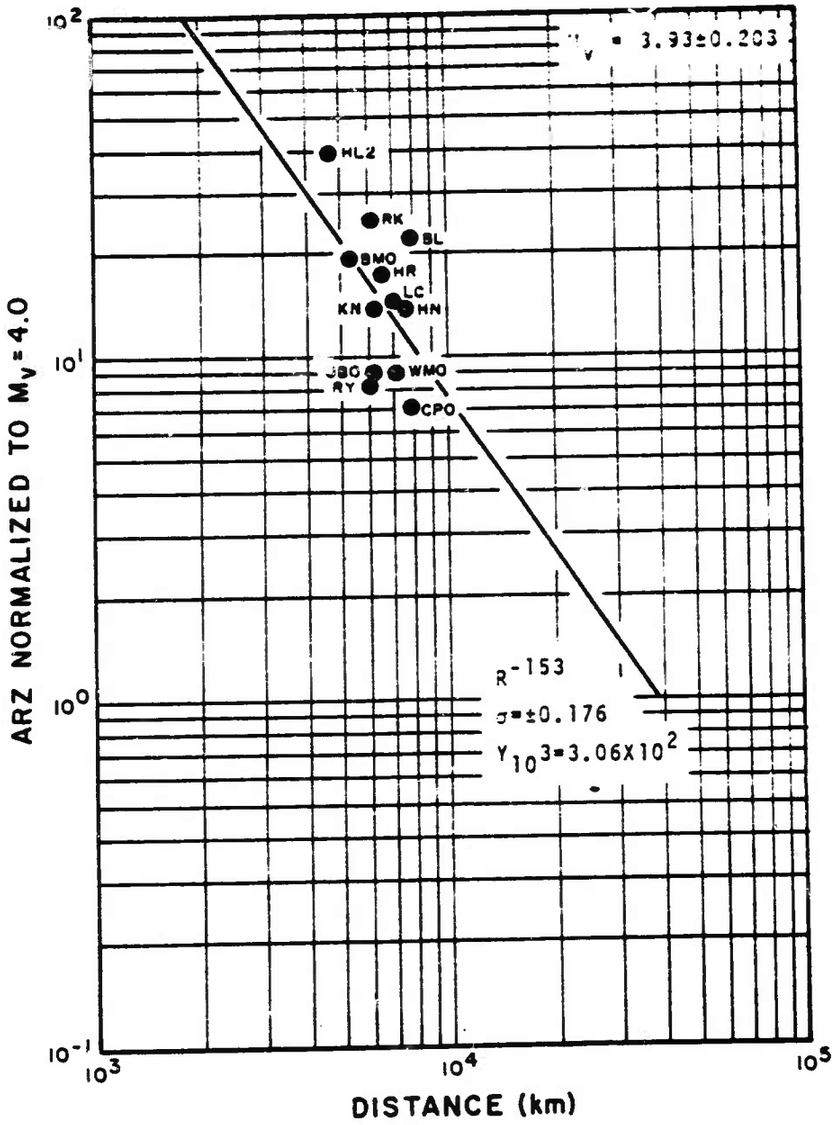

Figure 11a. Komandorsky Islands Eq. II - ARZ vs. Distance. Normalized to surface wave magnitude M_v = 4.0.

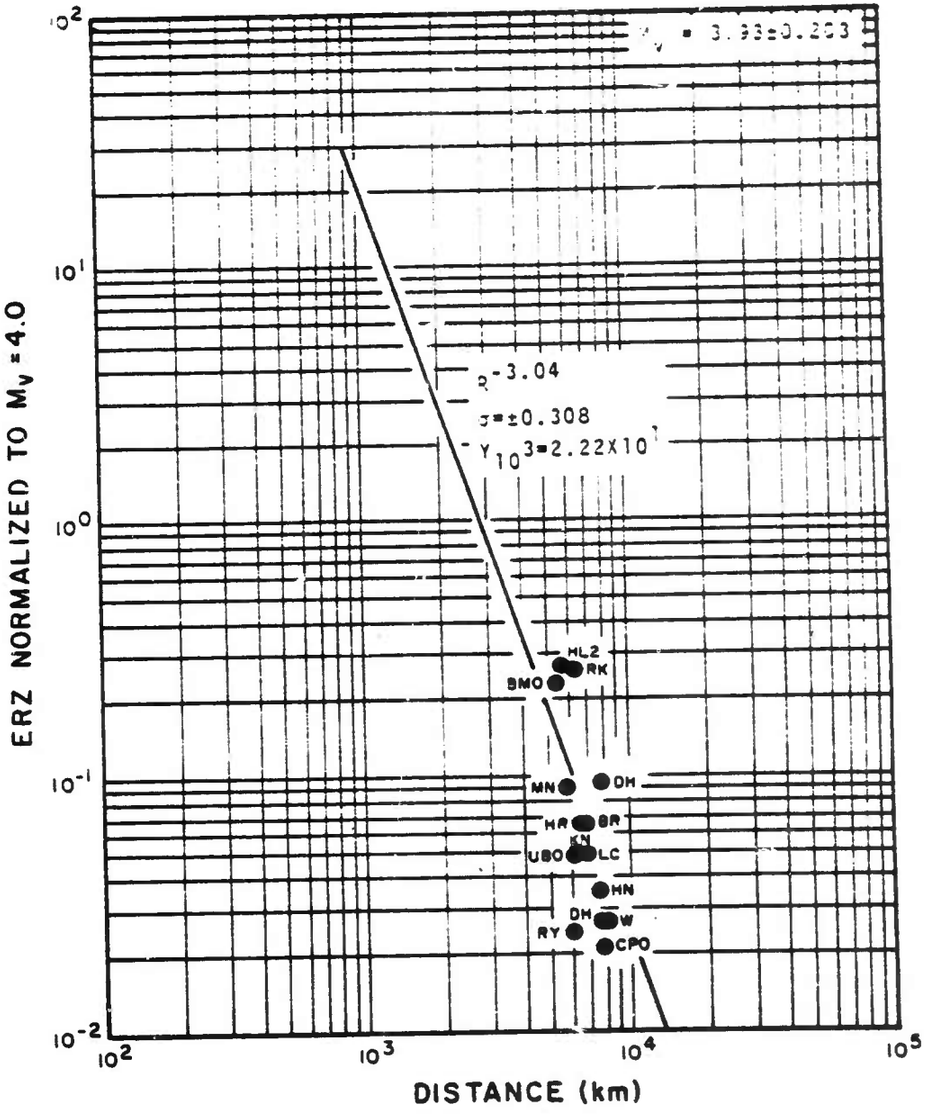

Figure 11b. Komandorsky Islands Eq. II - ERZ vs. Distance. Normalized to surface wave magnitude M_v = 4.0.

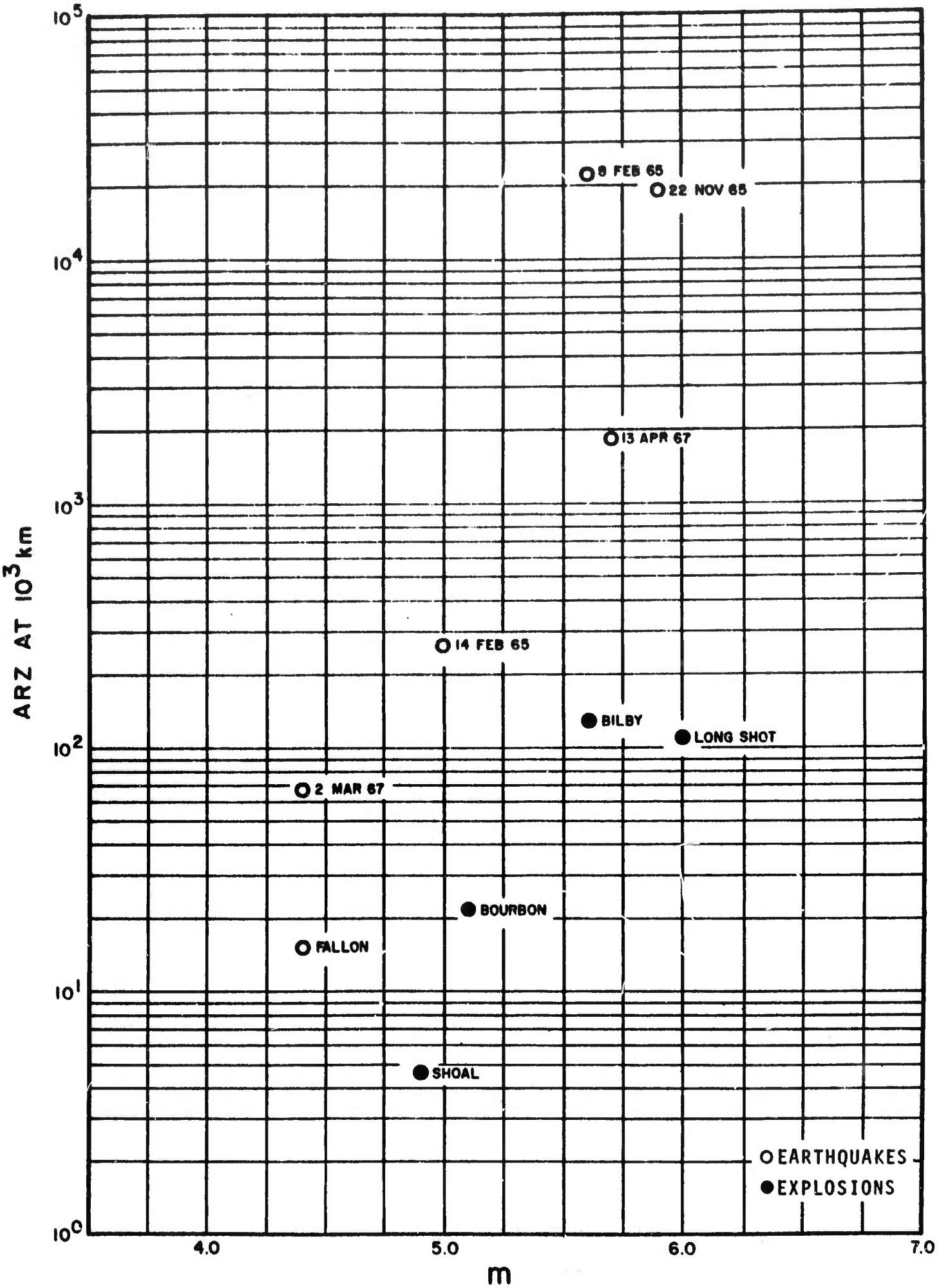

Figure 12. ARZ (At 1000 km) vs. P-wave magnitude (m_b) for 12 events.

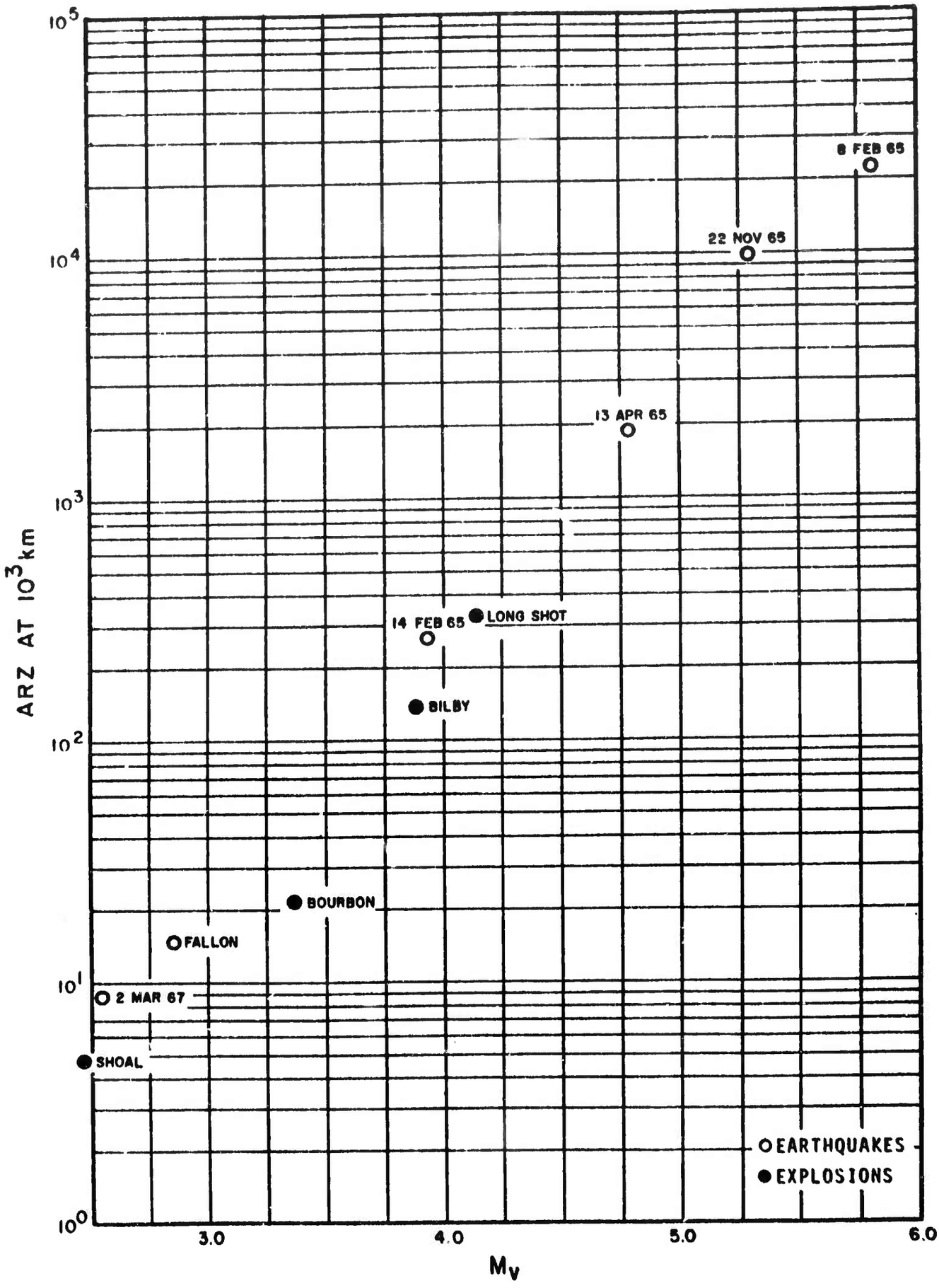

Figure 13. ARZ (At 1000 km) vs. Rayleigh wave magnitude (M_V) for 13 events.

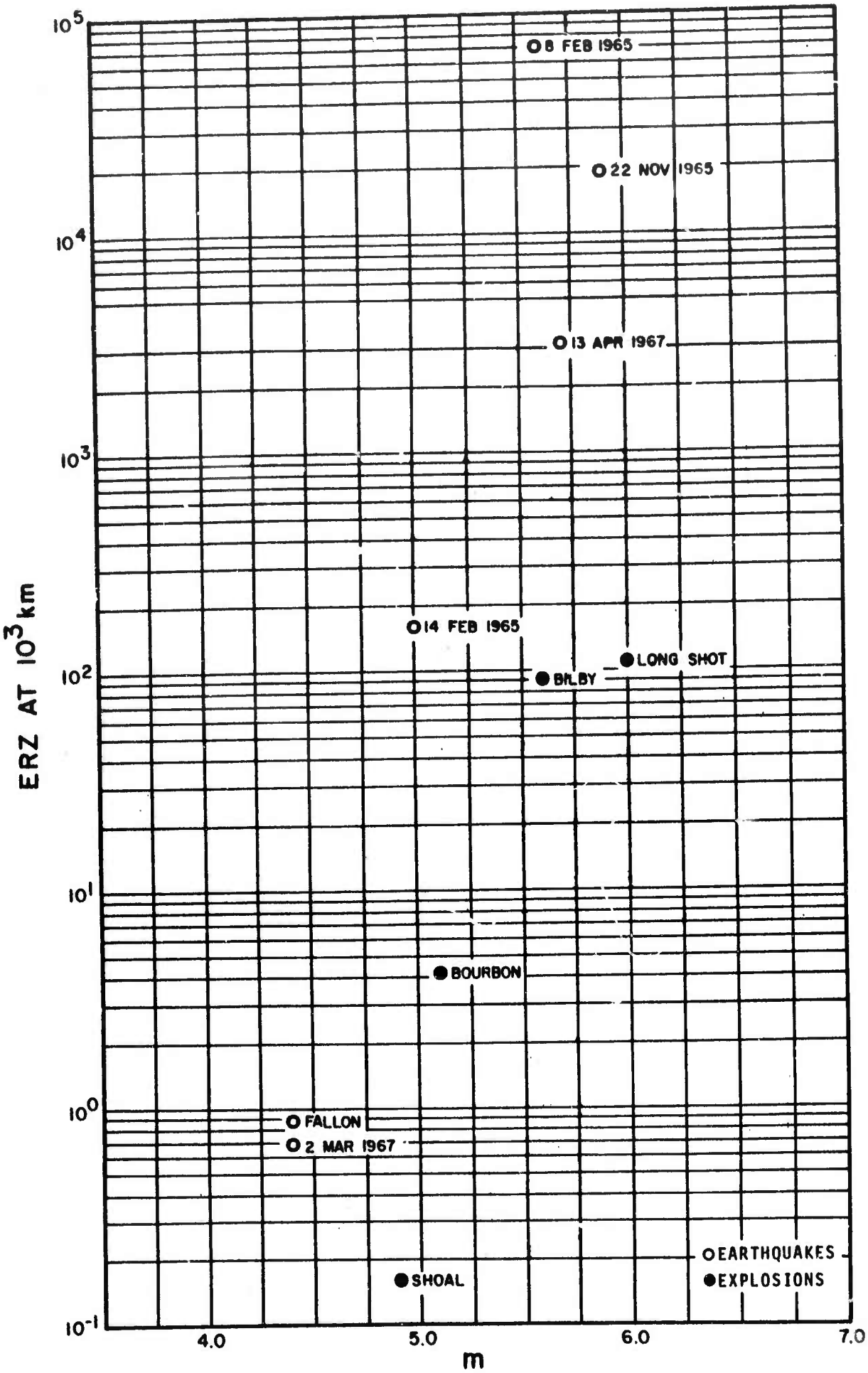

Figure 14. ERZ (At 1000 km) vs. P-wave magnitude (m_b) for 12 events.

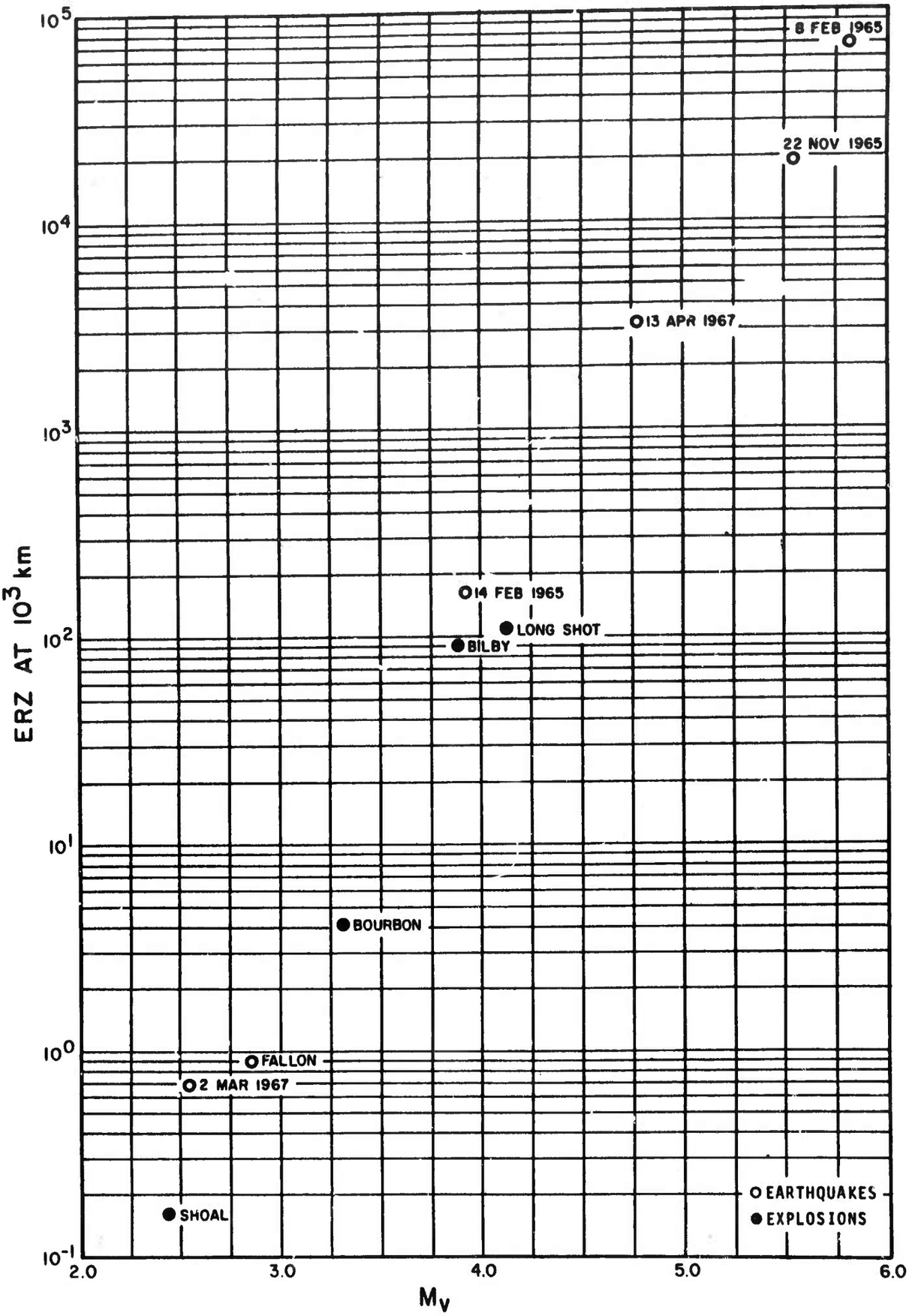

Figure 15. ERZ (At 1000 km) vs. Rayleigh wave magnitude (M_v) for 13 events.

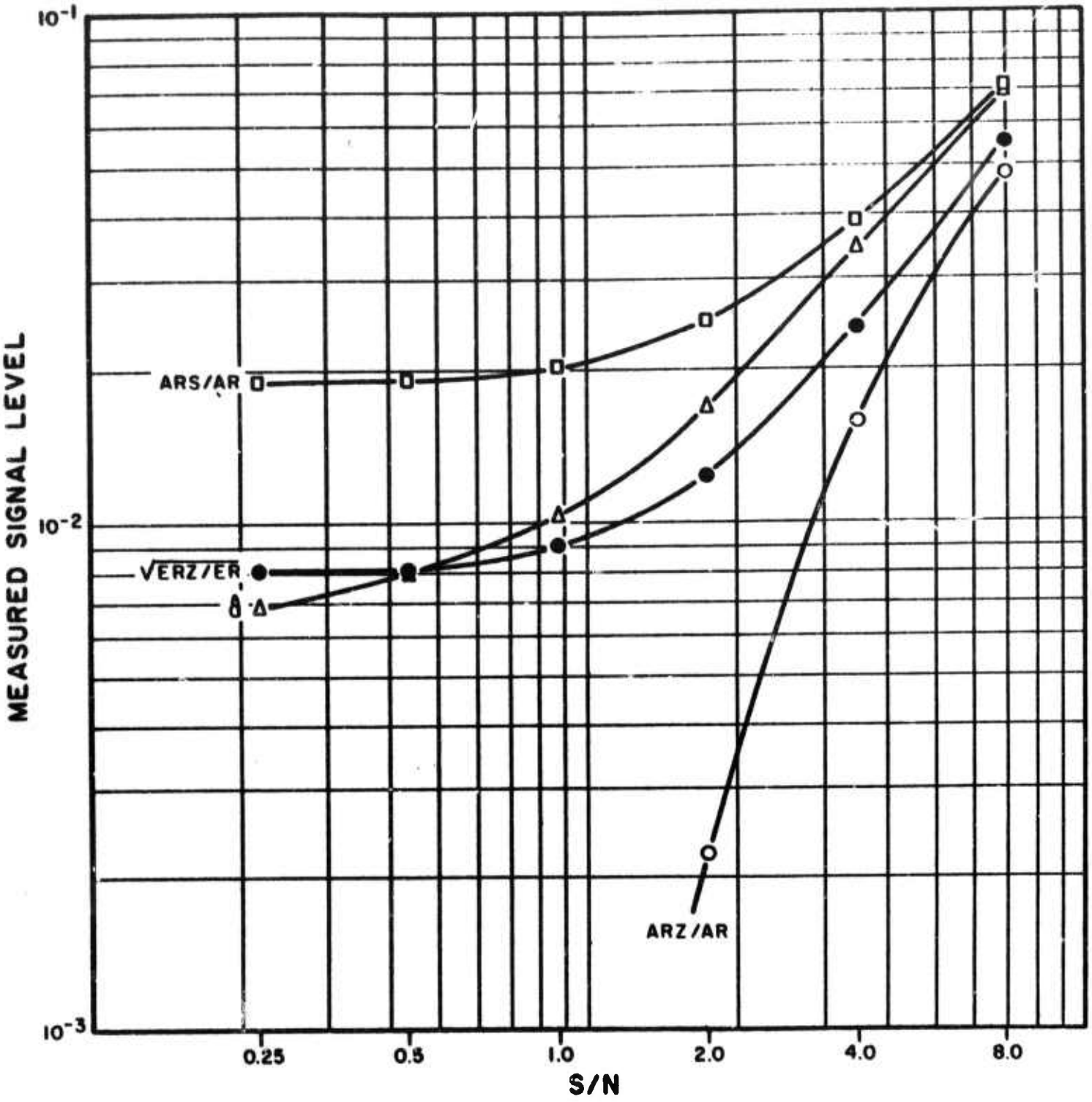

Figure 16. Comparison of data for synthetic case using matched filter and AR program - measured signal level vs. signal input level (S/N).

Unclassified

Security Classification

DOCUMENT CONTROL DATA - R&D

(Security classification of title, body of abstract and indexing annotation must be entered when the overall report is classified)

1 ORIGINATING ACTIVITY (Corporate author)
TELEDYNE, INC.
ALEXANDRIA, VIRGINIA

2a. REPORT SECURITY CLASSIFICATION
Unclassified

2b GROUP

3 REPORT TITLE
RAYLEIGH WAVE DISCRIMINATION TECHNIQUES BETWEEN UNDERGROUND EXPLOSIONS AND EARTHQUAKES

4 DESCRIPTIVE NOTES (Type of report and inclusive dates)
Scientific

5. AUTHOR(S) (Last name, first name, initial)
Turnbull,Jr., L.S.; Lambert, D.G.; Newton, C.A. (Pennsylvania State)

6. REPORT DATE
1 March 1968

7a. TOTAL NO. OF PAGES
42

7b. NO. OF REFS
8

8a. CONTRACT OR GRANT NO.
F 33657-68-C-0945

b. PROJECT NO.
VELA T/6702

c. ARPA Order 624

d. ARPA Program Code No. 8F10

9a. ORIGINATOR'S REPORT NUMBER(S)
211

9b. OTHER REPORT NO(S) (Any other numbers that may be assigned this report)

10 AVAILABILITY/LIMITATION NOTICES
This document is subject to special export controls and each transmittal to foreign governments or foreign nationals may be made only with prior approval of Chief, AFTAC.

11. SUPPLEMENTARY NOTES

12. SPONSORING MILITARY ACTIVITY
ADVANCED RESEARCH PROJECTS AGENCY
NUCLEAR TEST DETECTION OFFICE
WASHINGTON, D. C.

13 ABSTRACT

Discrimination between underground nuclear explosions and shallow earthquakes using the vertical component of the Rayleigh wave is achieved using several techniques. This analysis includes the previous developed area under the Rayleigh wave (ARZ), the newly applied total energy (ERZ) and the total energy transported across a unit width of the waveguide by the Rayleigh wave (REF). Results for several explosions and earthquakes of varying magnitudes are presented. Evaluation of these techniques and their applicability in an automated discrimination program is discussed. An attempt is made to incorporate a matched filter approach for weak signals.

14 KEY WORDS
Discrimination
Shallow Earthquakes and Explosions
ARZ
Matched Filter

Unclassified

Security Classification